SELECTIVE CATALYTIC OXIDATION OF HYDROGEN SULFIDE FROM SYNGAS

by

Huixing Li

B.S., South China University of Technology, 2003

M.S., Université de Savoie, 2006

Submitted to the Graduate Faculty of

Swanson School of Engineering in partial fulfillment

of the requirements for the degree of

Master of Science

University of Pittsburgh

2008

UNIVERSITY OF PITTSBURGH

SWANSON SCHOOL OF ENGINEERING

This thesis was presented

by

Huixing Li

It was defended on

April 1st, 2008

and approved by

Jason D. Monnell, Research Assistant Professor, Department of Civil & Environmental Engineering

Leonard W. Casson, Associate Professor, Department of Civil & Environmental Engineering

Thesis Advisor: Radisav D. Vidic, Professor and Chair, Department of Civil & Environmental Engineering

SELECTIVE CATALYTIC OXIDATION OF HYDROGEN SULFIDE FROM SYNGAS

Huixing Li, M.S.

University of Pittsburgh, 2008

In order to obtain a non-corrosive fuel gas (syngas), which is derived from coal by Integrated Gasification Combined Cycle (IGCC) technology and used in power plants, hydrogen sulfide (H_2S), which is generated during the gasification process due to sulfur contained in coal, should be removed to protect instruments, especially turbines, from corrosion. To improve H_2S removal efficiency and develop excellent regenerative catalyst, we conducted the following research. Simulated syngas was introduced into a fixed-bed quartz reactor where carbonaceous sorbents (which are excellent sorbents and have lower price) were positioned to capture H_2S. Tail gases from the outlet of the reactor including H_2S, COS, and SO_2 were continuously monitored by a residual gas analyzer (or mass spectrometer) to determine the capacity of H_2S uptake and selectivity of adsorption/oxidation by different sorbents.

Carbonaceous materials including carbon black, graphite and activated carbon fibers (ACFs) were compared for the application in desulfurization. Rare earth metal oxides (La_2O_3 and CeO_2) were investigated and used to modify ACFs due to their potential to effectively remove H_2S and multicycle regenerative ability. Water vapor and temperature effects on H_2S removal were studied.

Functional groups on carbonaceous materials were determined and the mechanism of the promotion of H_2S uptake by basic functional groups was proposed. Through the determination of activation energy of desorption of sulfur species from sulfided sorbents, it is concluded that

chemisorption is the dominant mechanism at higher sulfurization temperature, while physisorption is the controlling process at lower temperature. At the temperature ranging from 110 to 170 °C, the best H_2S-uptake capacity was obtained because chemisorption and physisorption are both present and water film on the surface of sorbents is ideally maintained. The observation of sulfurization and regeneration of sorbents and by-products related that nitrogen could only remove physically adsorbed H_2S and hydroxide could, to some extent, restrain the formation of by-products (the reaction between COS or SO_2 and hydroxide). ACFs modified by metal compounds showed excellent H_2S-uptake capacity (up to 35 mg H_2S/g Sorbent) in the 1st cycle but the capacity in the subsequent cycles were much lower than the 1st cycle because regeneration gas (nitrogen) could not recover the chemically adsorbed sulfur species.

Key words: Hydrogen Sulfide, Carbon, Syngas, Sulfurization, Adsorption, Regeneration

TABLE OF CONTENTS

LIST OF TABLES

LIST OF FIGURES

ACKLOWDEGMENT

I am grateful to my advisor Dr. Radisav D. Vidic for his teaching, advice and support in my research work. His precise research attitude, insight into different research field, social acceptability and wise leadership deeply impress me. I cannot be thankful enough to my research co-advisor Dr. Jason D. Monnell for participating in my research experiments, inspiring me, offering a variety of brilliant suggestions and solving a lot of problems.

I am thankful to Dr. Leonard W. Casson and Dr. Ronald Neufeld for their teaching. This study is supported by the National Energy Technology Laboratory (NETL), USDOE. I also wish to thank Maryanne Alvin from NETL, Esteban Broitman and Jim Miller from Carnegie Mellon University.

I would like to thank my colleagues and friends, Xihua Chen, Ravi Bhardwaj, Wei Sun and Kent Pu for their support and help on daily work and study. Last but not the least, great appreciation goes to my parents who show love and support to me.

1.0 INTRODUCTION

Hydrogen sulfide is an undesirable byproduct of using fossil fuels for energy since it is corrosive to process equipments. While the Clause process is able to remove up to 99% of H_2S, for fuel cell and syngas purpose, much more H_2S need to be removed. The presence of sulfur is a persistent problem related to fossil fuels and coal, and it must be removed before the fuels can be used as energy sources or chemical feedstock. The main usage of coal lies in generating electrical power and more than half of the total electricity in the U.S. is generated from coal. As our reliance on fossil fuels continues, coal will play a more and more important role because of its lower price [1]. Hydrogen sulfide (H_2S) exists naturally in many natural gas wells, and is produced largely in the desulfurization of petroleum stocks. For example, there are a few parts per million (ppm) to hundreds of ppm sulfur in gasoline or diesel fuels, up to 20 ppm sulfur in pipeline natural gas, several hundred ppm to more than 1.0% in coal-derived gaseous fuels (depending on the type of coal, the sulfur content in the feedstock, and the process). Though H_2S has a considerably high heating value, its use as a fuel is impossible because one of its combustion products is SO_2 which is harmful to environment due to the possibility to lead to acid rain. Further, H_2S is corrosive to power equipment and there is also sulfur deposition as well. When these fuels are used to produce hydrogen for proton exchange membrane (PEM) fuel cells, the sulfur content will severely poison fuel processing catalysts and platinum electrocatalysts.

Therefore, it is important and necessary to remove H_2S from these streams to allow further processing [2,3].

The integrated gasification combined cycle (IGCC) is considered to be the most efficient and environmentally acceptable technology for power generation from coal (Figure 1) [4]. The removal of pollutants from coal-derived fuel gas is needed for effectively using this technology. Among the pollutants, H_2S which is formed from sulfur contained in coal must be removed from the hot fuel gas not only to protect equipments against corrosion in the later stages of the process, but also to meet the environmental legislation for sulfur emissions [5].

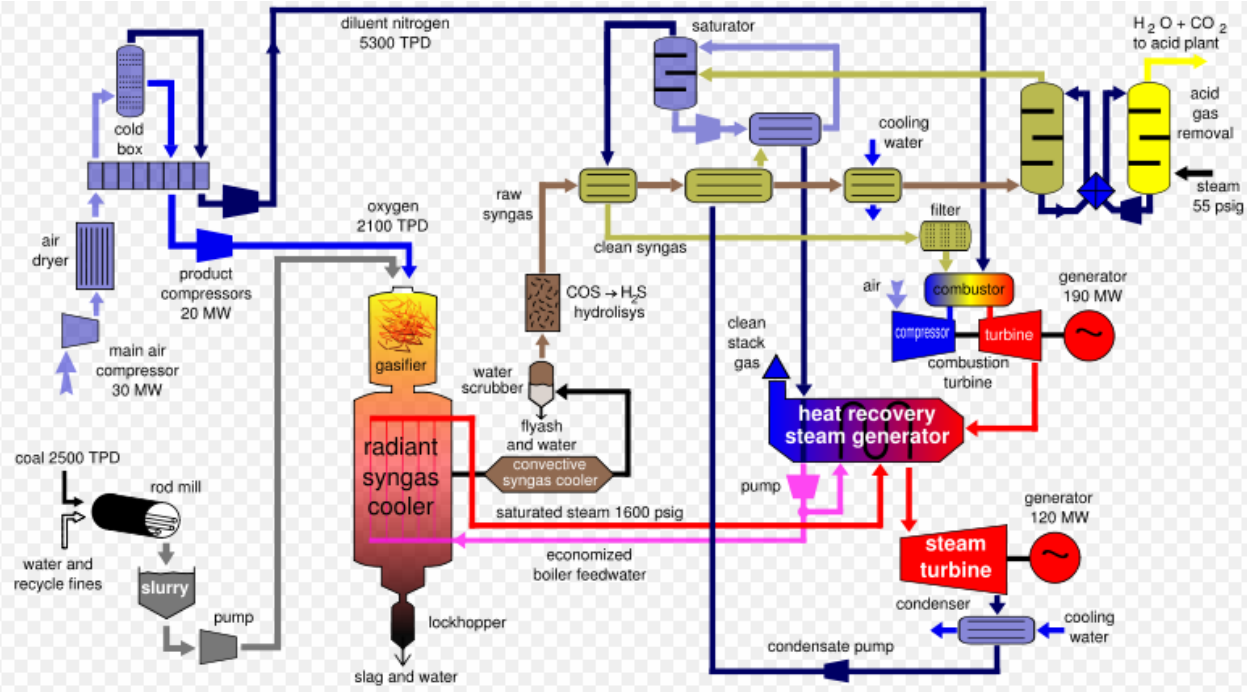

Figure 1. A schematic flow diagram of an IGCC plant. The gasification process can produce syngas from high-sulfur coal, heavy petroleum residues and biomass in a gasification unit. The gasification process produces heat, and this is reclaimed by steam "waste heat boilers". Steam turbines use this steam [4].

Syngas is a gas with abundance of CO and H_2, which are major components to generate electric power. Sulfur contained in the coal is transformed into H_2S and becomes part of

the syngas during coal gasification process. Therefore, H_2S needs to be removed from syngas before it is used to generate electric power because it is malodorous and corrosive.

There are many commercial treatment techniques that are used to remove H_2S including adsorption by activated carbon, condensation, chemical oxidation, incineration or catalytic combustion and dry/wet absorption. The disadvantage of these techniques is that hot coal gas (Generally, the temperature of syngas produced from coal gasification reaches 500 °C or above [6].) must be cooled down to ambient temperature or around 150 °C for desulfurization and then preheated to high temperature before being fed into gas turbine. In this way the thermal efficiency of the system is significantly reduced. It is for this reason that high temperature desulfurization technique has attracted more and more attention due to the fact that it can reduce H_2S down to 10 ppm level and avoid heat loss [6].

Porous materials show different activity and selectivity towards H_2S adsorption and/or oxidation. Zeolites show good activity at 300 °C, but they do not have good selectivity. Alumina and silica with macropores show both poor activity and selectivity. Metal oxides, especially V_2O_5, TiO_2, Fe_2O_3, CuO and ZnO show high activity for H_2S oxidation and regeneration capability [3].

Impregnated activated carbons have been used to remove H_2S efficiently. Alkaline materials such as NaOH, Na_2CO_3, KOH and K_2CO_3 were impregnated into activated carbons. It was found that the removal efficiency with these impregnated sorbents ranks as NaOH > Na_2CO_3 > KOH > K_2CO_3 [7].

Te regeneration of the spent sorbents remains a problem, since the material can degrade and lose its functional chemistry. For example, the thermal desorption of sulfur species from sulfided activated carbon, the formation of CO or CO_2 leads to the change of surface

characteristics of the initial carbon sorbent. On the other hand, the sulfur species are poorly removed by rinsing the activated carbons with water, because large amounts of sulfur species can remain trapped in pores due to the poor penetration of solvent [8]. Regeneration of spent carbon sorbents by thermal treatment with inert gas or gas mixture containing oxygen and/or water vapor is capable of partial regeneration of its initial capacity. This is due to the fact that elemental sulfur or sulfuric acid is strongly bound to active sites [9].

Given the limitation of current materials, it is necessary to develop H_2S-uptake sorbents with high removal efficiency, high catalytic activity, high selectivity for desired products and good regeneration ability. In this thesis, adsorption, oxidation and catalytic property of carbonaceous sorbents, impact of functional groups on carbon surface, effect of sulfurization temperature, water vapor and by-products, performance of rare earth metal modified sorbents and regeneration during H_2S removal process was investigated.

2.0 LITERATURE REVIEW

2.1 HYDROGEN SULFIDE SOURCES

H_2S is an undesired product of many industrial processes and it is primarily formed in nature by decomposition of organic materials by bacteria while it is also a constituent of natural gas, sulfur deposits, volcanic gases and sulfur springs [10]. Hydrogen sulfide (H_2S) is a toxic gas that can lead to personal distress even at a low concentration while at a higher concentration it can result in loss of consciousness, permanent brain damage or even death due to the neurotoxic effect [10].

In the Earth's past H_2S came from volcanic eruptions, which emitted CO_2 and methane into the atmosphere causing 'global warming'. Under elevated temperatures, the oceans were warmed resulting in lower dissolved oxygen, which would otherwise oxidize H_2S [11]. It is believed that volcanoes make the largest contribution of H_2S to the atmosphere from active and inactive volcanoes, as well as lava flows, domes, fumaroles, erupting lava and submarine hydrothermal areas. The major gas compositions include H_2O, SO_2 CO_2, and HCl, with minor components being N_2, H_2, CO, H_2S, HF and HBr. The gas composition is highly variable in terms of different locations and depends on the individual magma geochemistry and nature of an eruption [12].

H_2S exists in the biogeochemical cycle as the product of anaerobic oxidation by sulfur-reducing bacteria [11]. Anaerobic bacteria use sulfate as the electron acceptor in the

respiration process, resulting in the production of H_2S. They exist at a wide range of pH, pressure, temperature, and salinity conditions and are widely distributed in habitats. In anaerobic organic rich soils, H_2S is commonly present due to the reducing nature of the sediments and the precursor SO_4^{2-} is the second most common anion in seawater [12]. Bacteria break down organic matter produce H_2S. These microorganisms favor low-oxygen environments, such as in swamps and sewage.

Small amounts of H_2S exist in crude petroleum while up to 90% in natural gas. About 10% of total global emissions of H_2S are due to human activity including petroleum refineries, coke ovens, paper mills (using the sulfate method), and tanneries. Normal concentration of H_2S in clean air is about 100-200 ppb [11]. Burstyn et al. [13] conducted a survey of average concentrations of SO_2 and H_2S at rural locations in western Canada and determined that the average concentration is 0.1-0.2 ppb for H_2S, and 0.3-1.3 ppb for SO_2. The concentrations vary at different locations and are affected by seasons. Measured concentrations were affected by the wells, especially those within 2 km of monitoring stations. Locations close to sour gas wells and flares showed high H_2S concentrations and it is determined that oil and gas extraction activities contribute to air pollution in rural areas of western Canada.

IGCC plants produce large quantity of H_2S in coal-derived fuel gas. The commercial success of IGCC is greatly dependent on the accompanying air-pollution control systems. The success of such plants is essential because the IGCC technology with an efficiency of 52% is considered to be one of the key potential technologies that would meet the energy and environmental demands [1]. Table 1 shows the components of fuel gas or simulated fuel gas from different plants. From these values we determined a balance gas composition that was replicated for this study.

Table 1. Typical syngas compositions (% by volume). Syngas in this research was simulated according to the composition of syngas from NETL (the cooperator of this research).

Gas	H_2	CO	CO_2	H_2O	H_2S	N_2	O_2	Ref.
O-blown gasifier	27.7	39.4	13.1	18.4	1.1	0	0	[14]
Air-blown gasifier	14.2	23.1	5.8	6.6	0.5	49.8	0	[14]
Syngas stream	35	53	12	0	0	0	0	[15]
NETL Unshifted Gas	25-30	35-40	12-15	0.1-10	0.1-0.4	10-18	0.1-0.4	[16]
NETL Shifted Gas	45-50	0	34-38	0.07-7.4	0.28-0.3	11-12	0.28-0.3	[16]
This Thesis	24.4	34.6	15.2	0.4	0.4	16.8	0.4	

2.2 TECHNOLOGIES FOR H_2S REMOVAL

Many commercial technologies based on wet/dry adsorption and oxidation have been used for H_2S removal from gases. The Claus process, invented over 100 years ago, is the most significant gas desulfurizing process for recovering elemental sulfur from gaseous hydrogen sulfide (Figure 2) [17]. Dry catalytic processes based on the selective catalytic oxidation of H_2S to elemental sulfur have been developed [2]. Two dry Claus processes were developed to avoid the shortcoming of wet-Claus processes: Mobil's direct-oxidation process developed by Mobil AG Company in Germany and Super-Claus process developed by Comprimo Company in The Netherlands [18]. Both utilize one-step recovery of elemental sulfur from Claus tail gas by the following catalytic reaction:

$$H_2S + 1/2\ O_2 \rightarrow 1/n\ S_n + H_2O\ (n = 6 \sim 8)$$

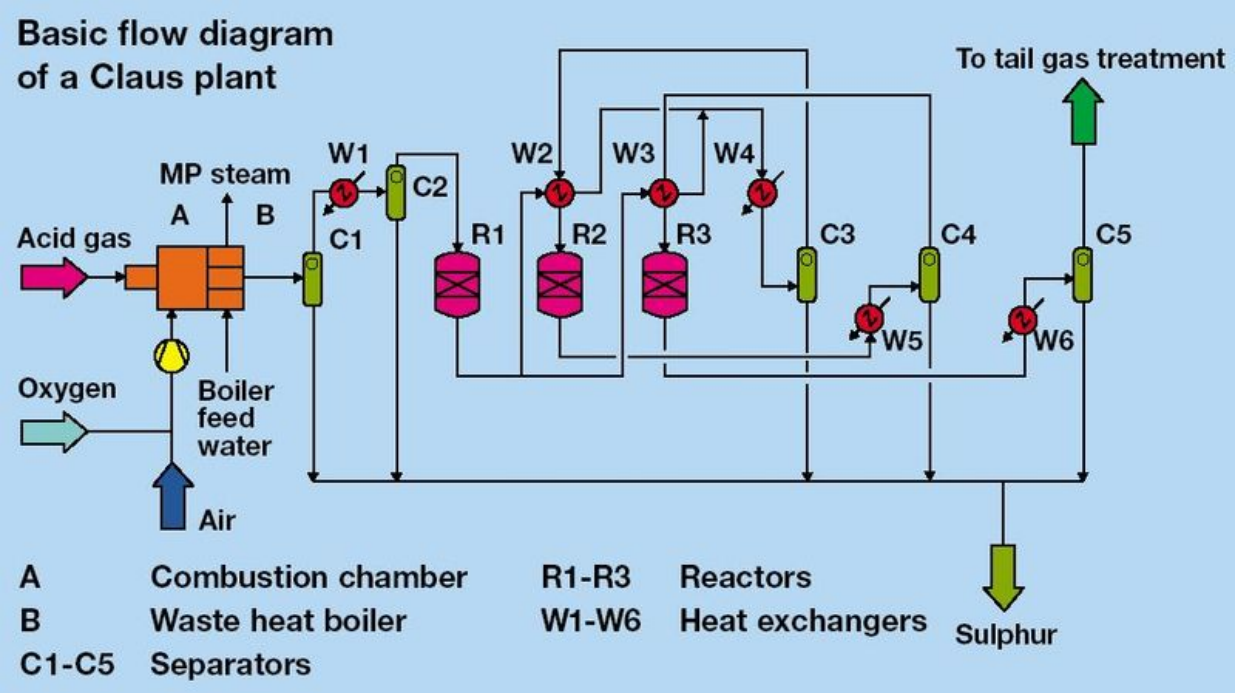

Figure 2. Schematic process flow diagram of a basic Claus process unit. The Claus technology can be divided into two process steps, thermal and catalytic. In the thermal step, H_2S-laden gas reacts in a substoichiometric combustion at temperatures above 850 °C such that elemental sulfur precipitates in the downstream process gas cooler. In the catalytic step the process continues with activated Al_2O_3 or TiO_2, and serves to boost the sulfur yield [17].

The catalyst used by Comprimo's Super-Claus process is alumina-supported iron oxide/chromium oxide, and the catalyst used by Mobil's direct-oxidation process is a TiO_2-based catalyst. However, there are some adverse portions of these processes, such as toxic properties of chromium oxide and the formation of SO_2 byproducts by way of the following reactions.

$$H_2S + 3/2\ O_2 \rightarrow SO_2 + H_2O$$

$$1/n\ S_n + O_2 \rightarrow SO_2$$

$$3/n\ S_n + 2\ H_2O \leftrightarrow 2\ H_2S + SO_2$$

Many factors that affect the selection of the gas-treating process have been investigated, including: the volume, temperature, and pressure of influent gas, space velocity, the selectivity required, the desirability of sulfur recovery, the types and concentrations of impurities present, surface characteristic of sorbents, the regeneration capability of sorbents, etc. [2].

The Claus process has high efficiency ranging from 94% to 97% and produce relatively small ecological impact when coupled with a tail-gas treatment unit. Moreover, its problems can be easily solved by using the correct stoichiometric amount of air, fuel gas, and acid feed gas. The capabilities of the conversion process have been improved, including innovations and optimization of process as well as reducing operating costs [2].

2.2.1 Use of Carbonaceous Based Materials to Remove H_2S

All carbon blacks (CB) have chemisorbed oxygen complexes (i.e., carboxylic, lactonic, phenolic groups, etc.) to varying degrees depending on the conditions of production. The high surface to volume ratio characteristic of CB structure leads to their special surface chemistry [19]. Carbon black is used principally for the reinforcement of rubber, as a black pigment in plastics, and for electrical conductivity.

Graphite is an electrical conductor and also is considered the highest grade of coal, although it is not normally used as fuel because it is hard to ignite. Graphite holds the distinction of being the most stable form of carbon under standard conditions. Therefore, it is used in thermochemistry as the standard state for defining the heat of formation of carbon compounds [20]. Kwon et al. [21] investigated oxygen- and hydrogen-containing functional groups on air-cleaved highly oriented pyrolytic graphite (HOPG) and plasma-oxidized HOPG. These groups almost completely suppress propane adsorption at 90 K. These groups can be removed by

thermal treatment (500 K) and lead to more than an order of magnitude increase in adsorption capacity. Morphological heterogeneity of plasma-oxidized HOPG provides larger surface area for adsorption as well as higher energy binding sites [21].

Activated carbons are excellent adsorbents with their specific application related to the properties of molecules to be removed/adsorbed. Microporous carbons favor the sorption/separation of light gases, while carbons with broad pore size distributions favor the removal of toxins or other large organic molecules. During the application of activated carbon, other features, such as surface chemistry, should also be taken into account [22].

Carbonaceous materials are commonly obtained from various organic precursors including peat, wood, coconut shells, polymers, etc.. During the process of physical activation, the precursor is carbonized at the temperature ranging 500 – 700 °C and then activated with steam or carbon dioxide at the temperature ranging 700 – 900 °C. During the process of chemical activation, different chemicals including phosphoric acid, zinc chloride or potassium hydroxide are mixed with the precursor and then carbonized under various temperatures. The different processing gives rise to many types of carbons with specific applications. Carbons are impregnated with chemicals such as KI, $KMnO_4$, KOH or NaOH to improve the efficiency of sorbents. Different manufacturing process produces activated carbons with different features, including surface area, porosity, surface chemistry, etc. [23].

The wide application of activated carbon is due to their large surface area (around 1000 m^2/ g) that supports many different chemistries, high pore volume, high density of carbon atoms in graphite-like layers, and their catalytic impact in various chemical reactions. The aforemention reasons that activated carbons could lead to fast and complete dissociation of hydrogen sulfide in basic environments and lead to its oxidation to elemental sulfur. A

combination of porosity and surface chemistry leads to the oxidation of hydrogen sulfide mainly to sulfuric acid which can be removed by water washing [23].

Bandosz et al. [24] used original activated carbons which were washed in a Soxhlet apparatus with distilled water to remove soluble components before sulfurization experiment to remove H_2S. Results of those experiments showed that surface functional groups containing oxygen, phosphorus and porosity of carbon significantly contribute to the process of H_2S remove. It was also found that functional groups present on the carbon surface act as catalyst for the oxidation of H_2S. Contact of physically adsorbed H_2S with adsorbed water probably results in oxidation of sulfur and formation of soluble sulfur species. The results show that neutral carbons, with developed microporosity which may enhance the physical sorption process performed worse as H_2S adsorbents on the basis of either volume or weight compared to the original carbons.

In general, activated carbons have micropores, mesopores and macropores hence the adsorption rate is limited by high diffusion resistance. While activated carbon fibers typically have micropores on the surface about 15 μm diameter fiber, the adsorption rate of activated carbon fibers is mostly controlled by rapid intraparticle diffusion so that diffusion resistance can be neglected [25].

Activated carbons are widely used as adsorbents of gases because of their large surface area and a big number of functional groups on their surface. When molecules are adsorbed on the carbon surface, they are bound by Van der Waals forces that work cooperatively in small pores. Moreover, the surface of activated carbons promotes catalytic/oxidative reactions due to the basic and acid functional groups thus aiding the adsorption and catalysis for H_2S oxidation [26].

ACFs (Figure 3) have special advantages compared to the usual granular activated carbon: (i) narrow pore size distribution, (ii) larger surface area, (iii) faster adsorption kinetics. In addition, their sulfur species adsorption capacity can be increased by the formation of suitable nitrogen-based surface groups via reaction with ammonia gas at high temperature [8]. Copper compounds have been found to aid ACF in increasing the adsorption capacity toward H_2S and COS [25].

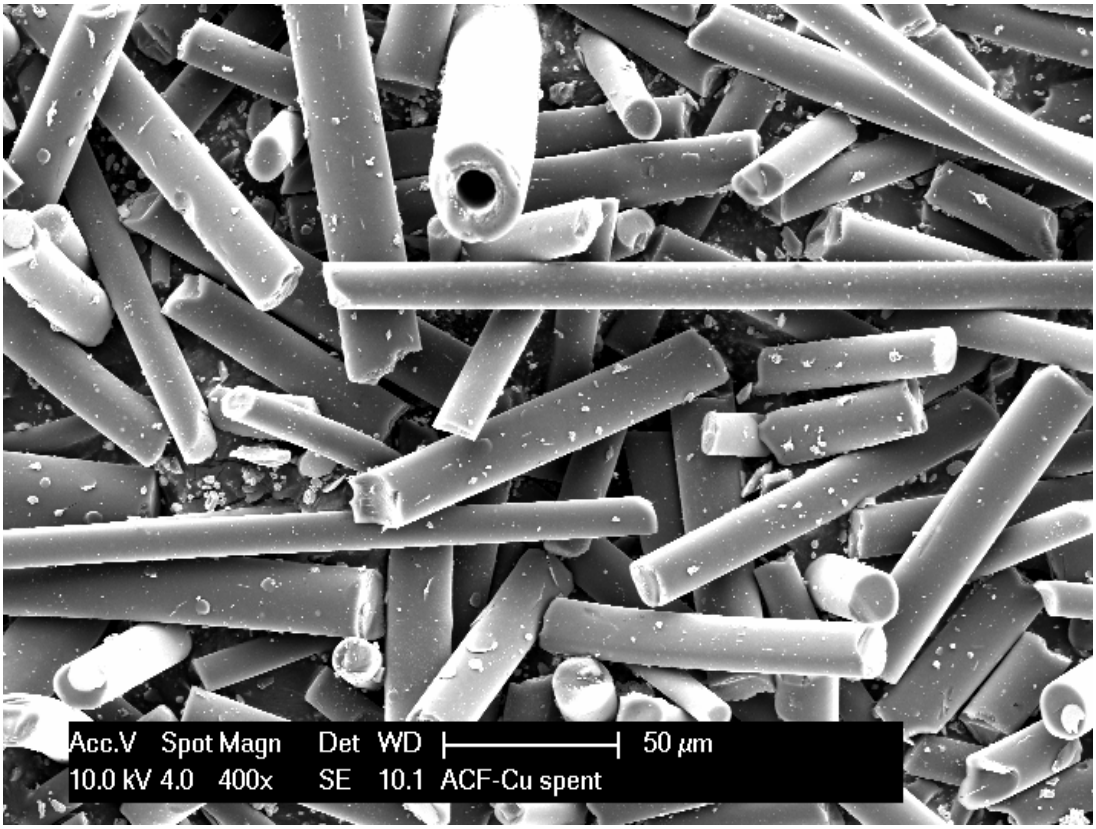

Figure 3. Scanning electron microscopy picture of activated carbon fibers used in this research. ACFs consist of long thin sheets of graphite-like carbon. A single ACF filament is a thin tube with a diameter of 5–8 micrometers and consists almost exclusively of carbon.

Several different chemicals have been used to impregnate sorbents to facilitate H_2S adsorption and catalytic breakdown including NaOH, KOH, Na_2CO_3, K_2CO_3 and KI [26]. It has

been observed that the H_2S breakthrough capacity increases 4-5 times with increasing loading of NaOH until maximum capacity is reached at about 10% NaOH. By increasing the pH value of the carbon, NaOH causes HS^- ion to be oxidized to elemental sulfur or sulfuric acid, until all of the NaOH reacts with H_2SO_4 [26]. However, this hydroxyl groups are completely used up and the capacity is lost without regeneration with more OH^-.

2.2.2 The Usage of Metal Oxide to Remove H_2S

Hee Kwon, et al. [5] mixed zinc oxide, titanium dioxide, nickel oxide, and cobalt oxide with an inorganic binder bentonite to fabricate Zn-Ti-based sorbents to remove H_2S. These sorbents showed excellent sulfur-removing capacities without deactivation even after 15 cycles of sulfurization and regeneration, while the conventional Zn-Ti sorbent deactivated easily. The nickel and cobalt in the sorbents worked as active sites during the sulfurization process, and also stabilized the sorbent structure to prevent a change of physical properties of the sorbents during multiple regenerations. The cobalt additive increased the regeneration capacity of the Zn-based sorbents by supplying heat to initiate the regeneration while the nickel additive prevented SO_2 slippage that originated from the cobalt sulfate.

One of the crucial factors for successful high-temperature desulfurization technology is effective removal of H_2S from fuel gases in the temperature ranging from 600 to 800 °C. Mixed metal oxides such as $ZnFe_2O_4$ can increase the H_2S removal efficiency and regenerability of the sorbent. ZnO-based sorbents could impart stability to ZnO against reduction to elemental zinc which causes undesired structural modifications of the sorbent in highly reducing coal gas streams. Besides ZnO-based sorbents, copper oxide that can be used at much higher temperature than ZnO has also been investigated [27].

Iron-containing catalysts are promising for the selective oxidation of H_2S. Fe and Fe/Cr catalysts supported on α-alumina or silica are used commercially as catalysts for the SUPERCLAUS process. When using iron-containing catalysts, the reaction selectivity decreases due to iron sulfide formation under the influence of the reaction medium. Through X-ray diffraction (XRD) and X-ray photoelectron spectroscopy (XPS), it was determined that iron disulfide FeS_2 is active in the oxidation of H_2S to SO_2 [28].

Rare earth elements include 15 lanthanide elements (La, Ce, Pr, Nd, Pm, Sm, Eu, Gd, Tb, Dy, Ho, Er, Tm, Yb, Lu) together with Sc and Y. The lanthanides have a wide range of applications [29]. Lanthanum and Ce (III) oxides, have excellent sulfidation thermodynamics in realistic reformate gas compositions, such as the ones produced by steam reforming, autothermal reforming, or partial oxidation of heavy oils, diesel, jet fuels, or by coal gasification [30].

Li et al. [29] investigated the catalytic oxidation of hydrogen sulfide to elemental sulfur on four rare earth orthovanadates (Ce, Y, La and Sm) and three magnesium vanadates (MgV_2O_6, $Mg_2V_2O_7$, and $Mg_3V_2O_8$). Among the rare earth orthovanadates, the sulfur yield decreased in the order $CeVO_4 > YVO_4 > SmVO_4 > LaVO_4$. It was found that sulfur yields of the rare earth orthovanadates and MgV_2O_6 were superior to those of vanadium oxide.

Flytzani-Stephanopoulos et al. [30] developed reversible adsorption of H_2S on cerium and lanthanum oxide surfaces over many cycles at temperatures up to 800 °C at very high space velocities to avoid bulk regeneration of the sorbent with its structural complexities. The adsorption and desorption processes are very fast, and removal of H_2S to a low level (< ppm) is achieved at very short (millisecond) contact times. Any type of sulfur-free gas, including water vapor, can be used to regenerate the sorbent surface. The capacity of H_2S uptake could reach 1.5 mg S/g Sorbent.

Table 2. Comparison of the application of metal oxides in desulfurization. Preparation methods of metal oxide catalysts, advantages and disadvantages in desulfurization with these catalysts are listed.

Metal	Preparation	Advantage	Disadvantage	Ref.
CaO	Calcination of $CaCO_3$	Can remove H_2S under high temperature and pressure	Earlier transition occurs at higher temperature	[6]
Ce	Support γ-Al_2O_3, SiO_2 and TiO_2 impregnated in $Ce(NO_3)_3$		Sorbent was converted to by-product Ce_2SO_2.	[6]
Co	Support γ-Al_2O_3, SiO_2 and TiO_2 impregnated in $Co(NO_3)_2$		High calcination temperature leads to formation of $CoAlO_4$.	[6]
Cu	Support γ-Al_2O_3, SiO_2 and TiO_2 impregnated in $Cu(NO_3)_2$	Can be used 100% in all temperature range		[6]
Cu	Bentonite binders	Able to migrate to carbon micropores and activate oxygen	Oxidation of H_2S to SO_2,	[31]
CuO and Cu_2O		Reduce H_2S from several thousand ppm to sub-ppm	Being reduced to elemental copper by the H_2 and CO contained in fuel gases Sintering of layers and causing structural degradation	[27]
$CuCr_2O_4$	Chromium nitrate mixed with a copper nitrate solution	Good tthermodynamic stability and slow reduction kinetics; Remove H_2S to less than 5-10 ppm at 650-850 °C		[27]

Table 2 (continued)

CuO-CeO2	Cerium nitrate mixed with copper nitrate solution	High H_2S removal efficiency, to less than 5-10 ppm at 650-850 °C	Easily reduce to CeO_{2-x},	[27]
Fe	Bentonite binders	An improvements in mechanical properties	Unable to activate oxygen	[31]
Fe	$Fe(NO_3)_3$ with silica	Catalysts calcined at higher temperatures are more stable against deactivation	Calcination at higher temperature reduces catalytic activity of catalysts in the H_2S oxidation	[28]
MgV_2O_6, $Mg_3V_2O_8$	$Mg(NO_3)_2{\cdot}6H_2O$ and NH_4VO_3, mixed with Sb_2O_4	Sulfur yields of magnesium vanadates improved significantly		[17]
Mn	Support γ-Al_2O_3, SiO_2 and TiO_2 impregnated in $Mn(NO_3)_2$	Can be used up to100% Reduction of Mn_2O_3 to Mn_3O_4 can provide additional energy to enhance H_2S sorption.		[6]
Zn	Support γ-Al_2O_3, SiO_2 and TiO_2 impregnated in $Zn(NO_3)_2$		Reduced to metallic zinc by H_2/CO and evaporate	[6]
Zn	Bentonite binders	An improvements in mechanical properties	Not able to activate oxygen	[31]
ZnO	$Zn(NO_3)_2$•6H2O	Muticycle tests of sulfidation and regeneration could be carried out	The rate of ZnO pellet sulfidation is limited by the internal mass transfer resistance	[32]
$ZnFe_2O_4$	Combining ZnO and Fe_2O_3		Component reduction at high temperatures	[27]
$ZnTi_xO_y$		Stable without reduction to elemental zinc at higher desulfurization		[27]

2.2.3 The Usage of Impregnated Sorbents to Remove H_2S

The amount of hydrogen sulfide adsorbed onto modified sorbents is larger than that adsorbed onto raw sorbents. The increase in the amount adsorbed onto modified sorbents may be due to the chemical interaction of the additives on the adsorbent and H_2S [33]. Impregnated sorbents have some disadvantages due to corrosive nature of impregnants such as KOH or NaOH [34].

Huang et al. [9] modified activated carbons via incipient wetness with copper nitrate solution. In terms of the impregnation process, they proposed the mechanism of reactions between impregnant solution and activated carbon shown in Figure 4. It was suggested that positive charges are attracted by the activated carbon surface leading to the increase in pH value of the solution. $Cu(OH)_2$ formed due to water dissociation shifts, depositing onto the surface of activated carbon. $Cu(OH)_2$ deposit plays an important role in catalysis and oxidation of H_2S.

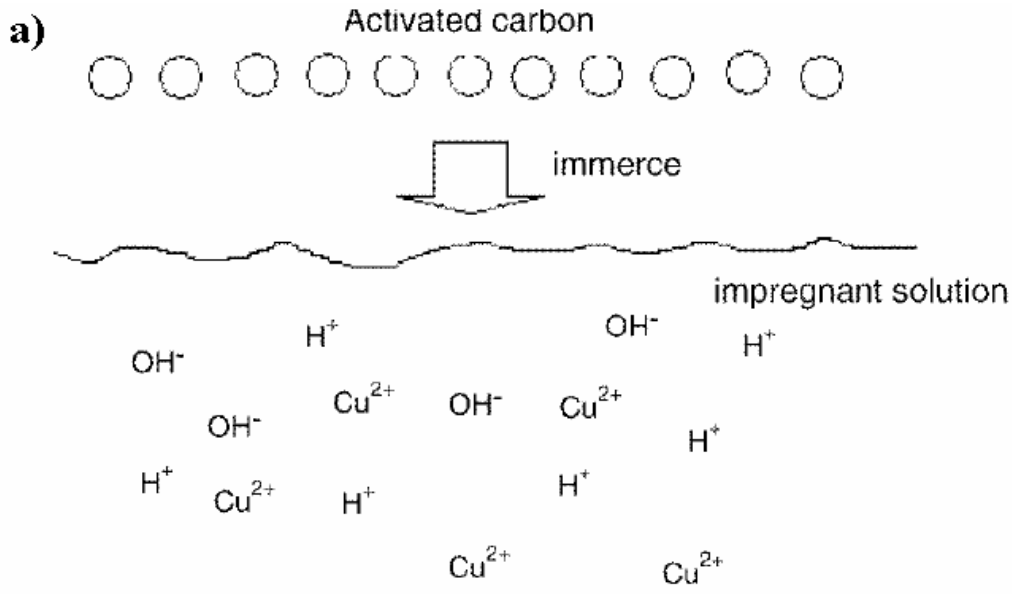

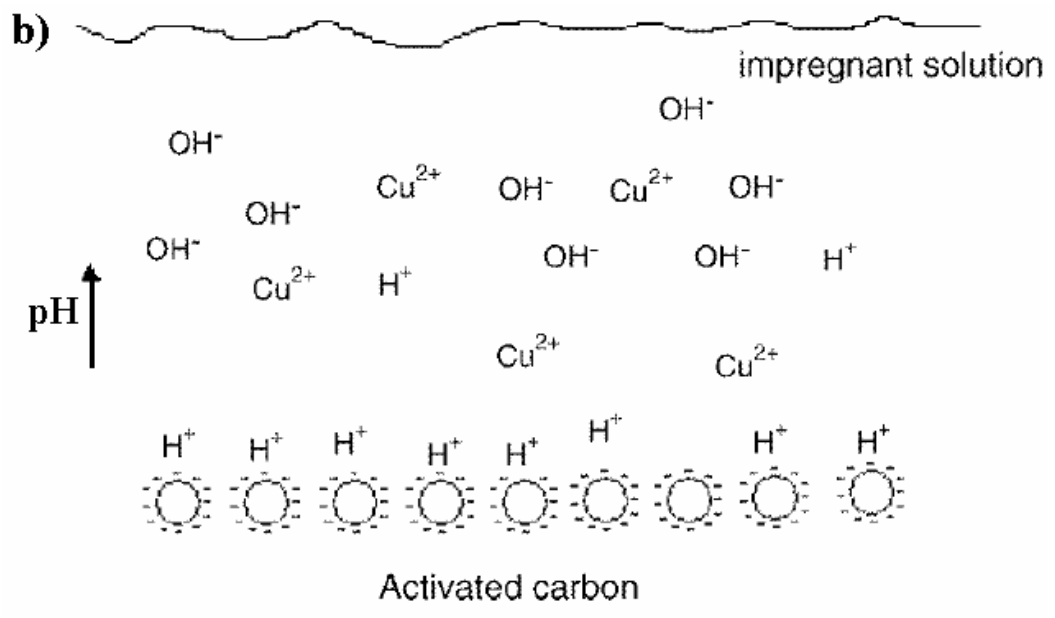
b)
impregnant solution
OH-
OH-
Cu2+
OH-
Cu2+
OH-
OH-
OH-
OH-
H+
Cu2+
H+
pH
Cu2+
Cu2+
H+
H+
H+
H+
H+
H+
H+
H+
Activated carbon

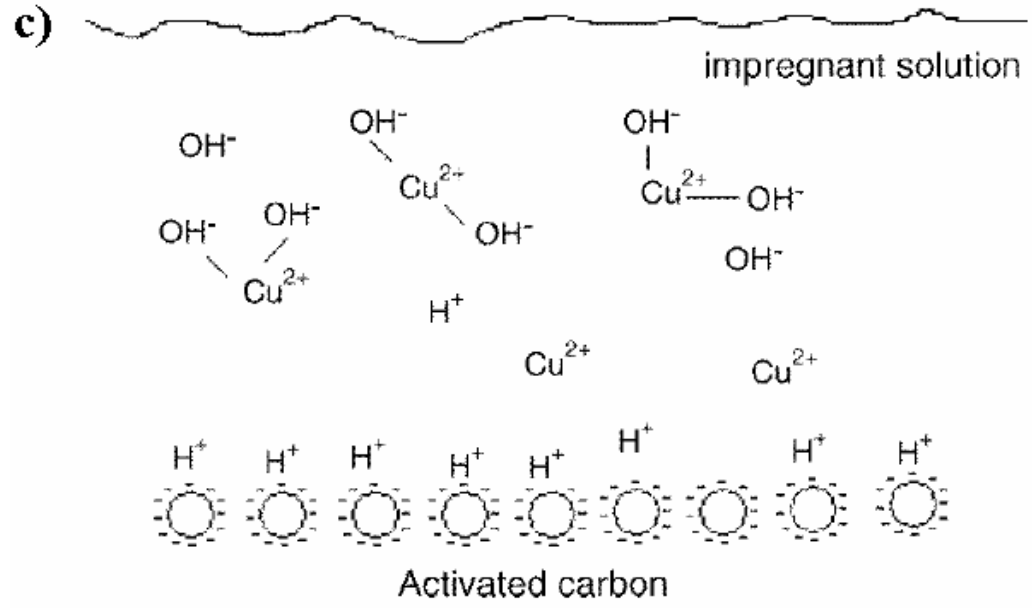
c)
impregnant solution
OH-
OH-
Cu2+
OH-
OH-
OH-
Cu2+
OH-
Cu2+
OH-
OH-
H+
Cu2+
Cu2+
H+
H+
H+
H+
H+
H+
H+
H+
Activated carbon

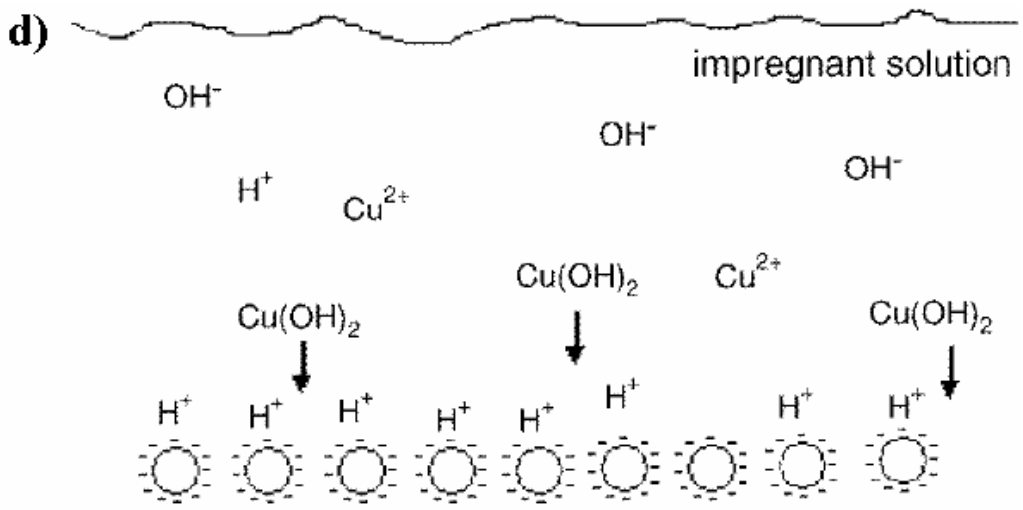

Figure 4. Schematic of movement between impregnated solution and sorbents: a) Copper nitrate dissociates to Cu^{2+} and NO_3^- ions in the solution which is used to impregnate activated carbons; b) the negative charge on the surface of unmodified activated carbon attracts H^+ ions in the solution resulting in pH increase of the solution; c) dissociated Cu^{2+} are attracted by activated carbon and combine with OH^- to form $Cu(OH)_2$; d) $Cu(OH)_2$ deposit onto the external surface and inside the pores of activated carbon [9].

Sorbents impregnated with caustic materials such as KOH and NaOH are widely used for adsorption of H_2S. The modification by impregnation of sorbents with metal hydroxide solutions resulted in a decrease in porosity, especially in micropore volume, because of adsorption or re-adsorption of metals in small pores [31]. Carbon support matrix actively adsorbs H_2S, which may greatly increase the H_2S removal efficient of sorbent [35]. Other way to increase H_2S adsorption capacity is through impregnation of carbons with oxidants such as KI or $KMnO_4$ which promote oxidation of H_2S to sulfur. The capacity for physical sorption of carbon may be

significantly decreased due to additive compounds because the micropores, which contribute to sorption efficiency are not available [24].

2.2.4 Other Methods to Remove H_2S

The well-developed physicochemical techniques typically used for the removal of H_2S have their advantages and disadvantages. Other alternations including a variety of biological desulfurization processes have been proposed including the use of phototrophic, heterotrophic and autotropic microorganisms. Various processes have been developed and compared based on the differences in nutritional requirements and abilities to catalyze specific reactions. Very few biological processes are flexible and rapid enough on a large scale, and much work related to the application of biological methods for treatment of H_2S still needs to be done [36]. One such method involving anaerobic, inorganic acid gas bioconversion though the photosynthetic van Niel reaction is shown in Figure 5 via a flow diagram for a phototrophic microbial acid gas bioconversion plant.

$$2n\ H_2S + n\ CO_2 \xrightarrow{(h\nu)} 2n\ S + n\ (CH_2O) + n\ H_2O$$

$$H_2S + 2\ CO_2 + 2\ H_2O \xrightarrow{(h\nu)} 2\ (CH_2O) + H_2SO_4$$

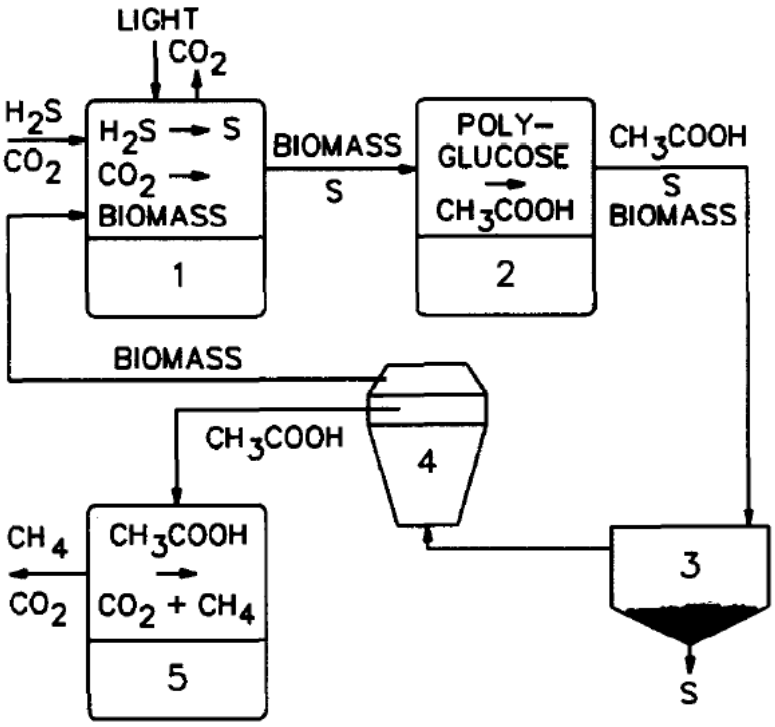

Figure 5. Flow diagram for a phototrophic microbial acid gas bioconversion plant, where 1, Photolithotrophic reactor; 2, dark reactor; 3, settler, 4, centrifuge; 5, anaerobic methane generation. [36].

More rapid and non-biological technologies are also being developed. For example, mesoporous materials can be generally used as adsorbents to remove impurities from gases. Melo et al. [37] studied the use of Zeolite 13X and Zinox 380 to remove H_2S at 25 °C. X-ray fluorescence and atomic absorption, X-ray diffraction, particle size distribution analyses and FT Infrared spectroscopy were employed to characterize these sorbents. The results show that both materials have promising future in the removal of H_2S from natural gas.

Demmink et al [38] studied the oxidative absorption of H_2S into the solutions of ferric chelates of ethylenediaminetetraacetic acid (EDTA) and hydroxyethylethylenediaminetriacetic acid (HEDTA) using a new penetration model for mass transfer parallel to chemical reaction. The absorption of H_2S into aqueous solutions is related the oxidation of H_2S:

$$H_2S\ (g) \rightleftharpoons H_2S\ (aq)$$

$$H_2S + 2Fe^{3+}L^{n-} \rightarrow 2Fe^{2+}L^{n-} + 2H^{+} + S \downarrow$$

where L^{n-} is an organic ligand, in this case ethylenediaminetetraacetic acid (EDTA, n = 4) and hydroxyethylethylenediaminetriacetic acid (HEDTA, n = 3). Limtrakul et al. [39] also used [Fe^{3+} EDTA] to remove H_2S (Figure 6). The removal reaction takes place in the riser and regeneration is performed in the downcomer. Iron (II) ethylenediaminetetraacetic acid [Fe^{2+} EDTA] could be regenerated to [Fe^{3+} EDTA] with a conversion of up to 79%. It was found that the conversion of H_2S decreased with increasing superficial gas velocity in the riser, which is due to the decrease in the liquid-phase circulation time. Desulfurization and regeneration can be carried out in the same vessel, which would reduce the capital costs. H_2S is injected at the bottom of the riser, where the reaction occurs, and injecting air in the downcomer for catalyst regeneration or vice versa. The gas holdup in the riser is more than that in the downcomer, and the resulting density or pressure difference leads to a natural liquid circulation from the downcomer the riser without any pump. The gas-lift reactor is economical and has no moving parts.

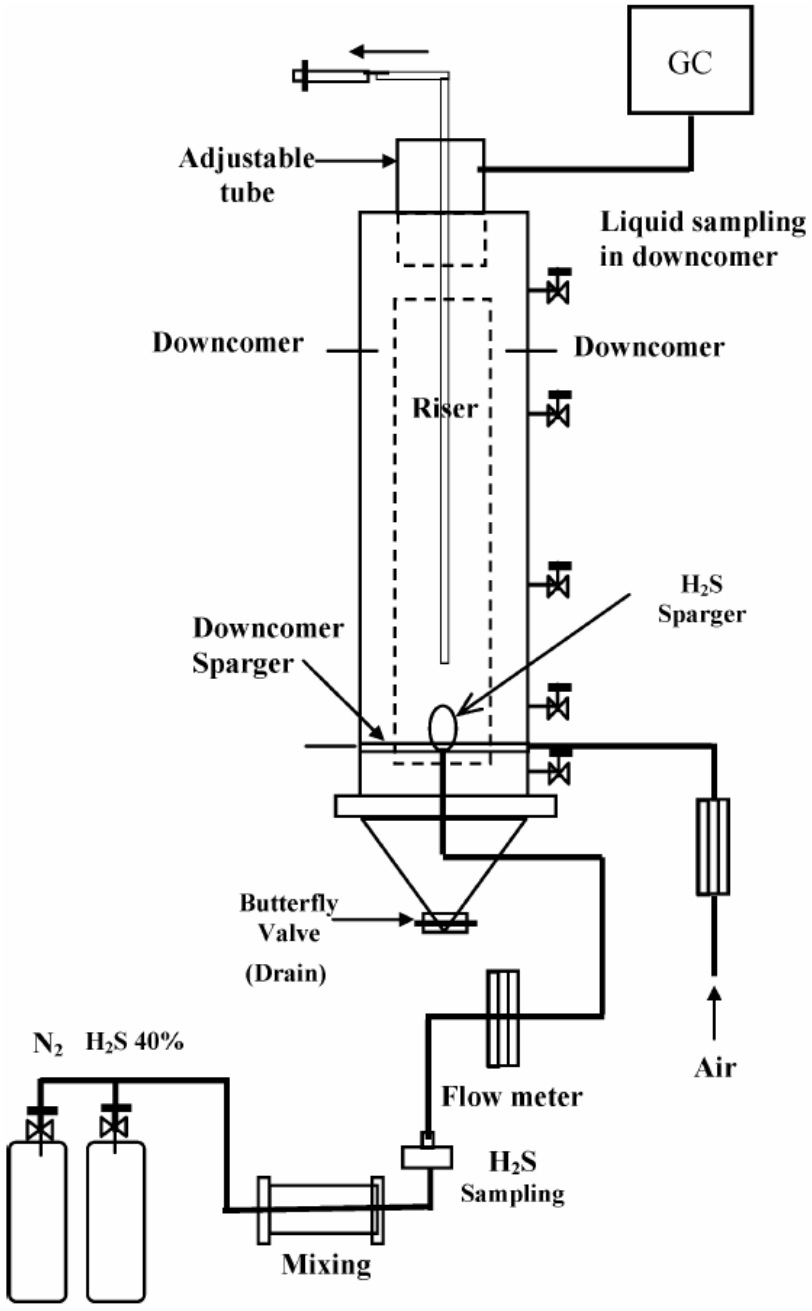

Figure 6. Gas-lift reactor where H_2S is injected at the bottom of the riser and air injected in the downcomer for catalyst regeneration. The removal reaction takes place in the riser and regeneration is performed in the downcomer. H_2S is injected at the bottom of the riser, where the reaction occurs, and injecting air in the downcomer for catalyst regeneration [39].

2.3 EFFECT OF PROCESS CONDITIONS ON H_2S REMOVAL

During the process of removing H_2S, there are two main kinetic steps. The first is controlled by oxidation/adsorption reaction while the second is controlled by the by-products which reduce the carbon site accessibility [34]. In the first step, the amount of water introduced, sulfurization temperature, pressure of influent gas mixture, amount of catalysts used, and so forth can affect the H_2S removal efficiency. In terms of catalyst, the surface area, pore width, pore volume, and functional groups on catalysts have certain effect on H_2S adsorption/oxidation.

Bashkova et al. [40] found that the selectivity for oxidation of H_2S to elemental sulfur is dependent on the textural, structural, and chemical characteristics of the carbon catalyst. Catalytically-active nitrogen species in the carbon postponed breakthrough time and increased capacity for H_2S uptake but inversely catalyzed the early formation of SO_2 and COS into the treated fuel gas stream. The significant micropore volume and narrow pore width of carbon aid the capture of elemental sulfur and SO_2 formed and the retaining of these oxidation products for a longer time. Furthermore, they found that activated carbon could convert COS to sulfur due to a large amount of highly reactive basic groups on the carbon surface.

2.3.1 Water Vapor Effects

The role of the humidity is highly beneficial for the removal of hydrogen sulfide as it removes the by-products formed. Trace water in process gases leads to the acidification of the carbon surface in the presence of oxygen or carbon dioxide, and hence restrains the dissociation of hydrogen sulfide. Under humid condition, the oxygen or carbon dioxide results in a faster

reaction kinetic. The acidification of the carbon surface is counterbalanced by the dissolution of the by-products [34].

The inlet gas containing humidity leads to the condensation of water in the pore structure resulting in dissolution of O_2 and H_2S gases into the water film where oxidation of H_2S subsequently happens. The HS^- ions and O_2 diffuse inside a thin water film, which increases with the polar groups present on the surface due to the formation of hydrogen bonds between the polar species and adsorbed water. Single water molecules are adsorbed on the boundary surface. The dissolution of H_2S to HS^- is related to the amounts of water and the pH value of the water film. Acidic carbon surface reduces the dissociation of H_2S to HS^- ions while basic carbon surface promotes the dissociation of H_2S to HS^- ions. Basic condition results in a higher concentration of HS^- ions, which are then oxidized to sulfur polymers having a chain or ring-like structure [41].

The presence of moisture in gas stream plays an important role as a medium to enhance oxidation of H_2S. The dissolved H_2S reacts with O_2 and converts to sulfur species in the water film on the surface of carbon. Under moisture atmosphere, additive metal oxides could oxidize H_2S though competition of adsorption may occur [9].

Under dry condition the adsorbed H_2S is oxidized in a substitution reaction by oxygen functional groups present on the carbon surface. Under wet condition, the reaction pathway begins by the dissolution of H_2S and oxygen in a thin water film on the adsorbent surface or in the pores and is followed by a radical oxidation reaction. The highest adsorption capacity could be obtained under a wet air atmosphere with the strongest basic carbon material [41].

Huang et al. [9] conducted parallel experiments of sulfurization of activated carbons (impregnated by $Cu(NO_3)_2$) with gas mixture containing different relative humidity, including 0, 40-50% and 70-80%. They observed that the H_2S uptake capacity decreased with the increase in

relative humidity. Such behavior is attributed to the competition of adsorption between H_2S and H_2O on the surface of sorbent. Adsorption is an exothermic process which leads to the difficulty of condensing water vapor to form water film [9].

2.3.2 Temperature and Surface Area Effect

Bukhtiyarova et al. [28] studied the effect of the calcination temperature on the iron oxide catalysts prepared by impregnation of silica with iron (III) nitrate for H_2S oxidation. It was found that the increase in the calcination temperature decreases the catalytic activity of the Fe_2O_3/SiO_2 catalysts in H_2S oxidation, which has been ascribed to the agglomeration of iron oxide particles and a subsequent decrease in active surface sites. However, the increase in the calcination temperature makes the catalyst more stable towards the sulfidation of Fe_2O_3 to iron disulfide phase.

ACFs are highly microporous solids with a small external surface area and very little mesoporosity. Ishii et al. [42] found that the surface area of ACF decreases with the increase in treatment temperature (1200 °C). The surface area of ACF decreased from 1460 m^2/g to 780 m^2/g and treated ACF has slit-shaped micropores due to micrographitic structures. Heat pretreatment of ACFs is believed to remove functional groups on the carbon surface and create additional surface area, which is helpful to adsorption [43]. However, increasing the treatment temperature decreases the adsorption capacity of ACF due to the collapse of micropores [42]. The high temperature treatment could partially gasify the micropore walls and thus increase the micropore width. Nevertheless, some micropores become closed pores with reconstruction of micrographitic structure in crystal growth leading to micropore volume decreased [42].

Chauk et al. [1] used CaO, which was obtained from calcination of $CaCO_3$, to remove H_2S at the temperature ranging from 650 °C to 900 °C. It was found that sulfidation conversion is very sensitive to reaction temperature and the rate of sulfidation at the beginning increased significantly with temperatures. At higher temperature, the tapering off of the overall reaction rate is more drastic than that at relatively lower temperatures. In the beginning, the surface reaction may control the overall rate of CaO sulfidation. The rate of surface reaction increases exponentially with temperature so that the nonporous CaS product layer builds up and occupies pores leading to a decrease in the porosity of CaO. Therefore, diffusion resistance increases and product layer diffusion begins to control the overall rate of H_2S uptake.

Cal et al. [35] studied the effect of temperature on H_2S adsorption at lower temperature (400-600 °C) with Zn-impregnated carbon sorbents. They found that the temperature difference in this range had no effect on breakthrough time, which was ascribed to principles of chemical adsorption that required a certain amount of activation energy. Physical adsorption of H_2S remains constant at lower temperatures (< 550 °C).

Desulfurization at much lower temperature (23-25 °C) was studied using inexpensive-waste-based sorbent such as wood or coal fly ash. For example, elemental sulfur was the end product of H_2S oxidation but the catalytic decay occurred due to surface pores being occupied by elemental sulfur and associated reduction in surface area (44.9-1.4 m^2/g) of fly ash. Catalyst regeneration with hot water (85 °C) washing was elevated, but only half of the original H_2S oxidation activity could be regenerated [44].

2.3.3 Impact of Surface Functional Groups

Several methods have been used to detect and quantify oxygen functional groups on carbon surfaces, such as Infrared spectroscopy (IR), X-ray photoelectron spectroscopy (XPS), thermal desorption spectroscopy (TPD), elemental analysis and Boehm titration [45]. Oxygen-containing sites exist in the form of organic functional groups, which can be acidic, basic, or neutral, and could be catalytic centers for H_2S oxidation. The H_2S removal capacities are enhanced by the presence of these oxygen functional groups [41].

Feng et al. [45] used covalent fluorescent labeling of surface species (FLOSS) to detect relatively low amounts of surface functional groups (OH, COOH and CHO) on activated carbon fiber surfaces. The chromophores were attached to the surface through reaction with each type of surface functional group. FLOSS indicated the presence of COOH and CHO groups on the ACF fiber surface while the infrared spectrum and the X-ray photoelectron spectrum could not detect the existence of such few groups. However FLOSS could only detect exposed functional groups and not functional groups inside smaller pores.

Spatial location, strength of interaction, and availability of surface oxygen groups are important parameters in determining the dynamic adsorption performance of the carbons. The total acidity, including carboxylic, lactonic and phenolic groups present on each carbon surface, increases after oxidation and it leads to the decrease of H_2S capture [46].

All oxygen groups on the carbon surface act as catalysts for the oxidation reaction, but the basic groups play a more significant role in the process of H_2S adsorption because basic surface ensures a better immobilization of H_2S molecules. H_2S is an acidic gas and the presence of basic groups contributes to the immobilization process. Thus the local pH in the pore structure

affects H_2S adsorption/oxidation and the basic oxygen functional group concentration is an important parameter for H_2S uptake [41].

2.4 MECHANISM OF H_2S REMOVAL BY CATALYTIC REACTIONS

The Claus reaction has been the standard method used in industry to remove H_2S from waste/process gas streams. It is well known that the following basic reactions occur in the Claus process [6]:

$$2\ H_2S + O_2 \rightarrow (2/n)\ S_n + 2\ H_2O$$

$$(1/n)\ S_n + O_2 \rightarrow SO_2$$

$$2\ H_2S + 3O_2 \rightarrow 2\ SO_2 + 2\ H_2O$$

$$2\ H_2S + SO_2 \leftrightarrow (3/n)\ S_n \downarrow + 2\ H_2O$$

Ammonia which is a basic compound is also used to react with H_2S to form ammonium sulfide $[(NH_4)_2S]$ which can be oxidized to produce elemental sulfur [6]:

$$H_2S + 2\ NH_3 \leftrightarrow (NH_4)_2S$$

$$(NH_4)_2S + (1/2)\ O_2 \rightarrow S \downarrow + 2\ NH_3 + H_2O$$

When NaOH [26] is used to impregnate activated carbons, NaOH shifts the dissociation of hydrogen sulfide forward, thus increasing concentration of HS^- ions where K_{a1}=9.6 x 10^{-8} and K_{a2}= 13 x 10^{-14}, shown as below

$$H_2S \overset{K_{a1}}{\rightleftharpoons} HS^- \overset{K_{a2}}{\rightleftharpoons} S^{2-}$$

HS^- ion is promotes oxidation of hydrogen sulfide to elemental sulfur, SO_2 or sulfuric acid in the presence of water. In addition, elemental sulfur, S_x, or polysulfides, HS_xSH, deposited on carbon might be active sites for H_2S oxidation and catalyze the process.

$$H_2S + 0.5O_2 \rightarrow S + H_2O$$
$$S_x + H_2S \rightarrow HS_xSH$$
$$HS_xSH \rightarrow HS_xS\bullet + H\bullet$$
$$HS_xS\bullet + 0.5O_2 \rightarrow HS_xS(O)$$
$$HS_xS(O) + H_2S \rightarrow HS_{x+1}S\bullet + H_2O$$
$$HS_xS(O) + 0.5O_2 \rightarrow HS_{x-1}S\bullet + SO_2$$
$$SO_2 + 0.5O_2 + H_2O \rightarrow H_2SO_4$$
$$2H_2S + SO_2 \rightarrow 3S + 2H_2O$$

On the surface of NaOH-impregnated carbon

$$NaOH + H_2S \rightarrow NaHS + H_2O$$
$$2NaOH + H_2S \rightarrow Na_2S + H_2O$$
$$NaHS + 0.5O_2 \rightarrow S + NaOH$$
$$Na_2S + 0.5O_2 + H_2O \rightarrow S + 2NaOH$$
$$2NaOH + H_2SO_4 \rightarrow Na_2SO_4 + 2H_2O$$

Cal et al. [35] suggested that there are mainly three possible reactions for H_2S uptake by carbon-based metal-containing sorbents (involving carbon support, oxygen-containing active sites and additive metal), as shown below:

1) Carbon: adsorption reaction between sulfur and carbon active sites, which could be identified by oxygen desorption.

$$C + H_2S \rightarrow C\text{-}S + H_2$$

2) Carbon–oxygen sites: a substitution reaction in which sulfur replaces oxygen in the carbon–oxygen bond. Higher surface-oxygen density leads to greater possibility of this substitution reaction.

$$C\text{-}O + H_2S \rightarrow C\text{-}S + H_2O$$

3) Metal: reaction between sulfur and active metal because H_2S is very reactive with some metals.

$$C\text{-}M + H_2S \rightarrow C\text{-}M\text{-}S + H_2$$

The proposed mechanism of the adsorption of H_2S on Pt anodes proceeds through instant dissociation of H_2S on the Pt to produce Pt–S species [47].

$$H_2S + Pt \rightarrow Pt\text{-}S + H_2$$

The amount of sulfate formed is so small that it could be negligible for ordinary process. However, for fuel cells they will eventually kill the catalysts and render them useless.

$$H_2S + 4\ H_2O \rightarrow SO_4^{2-} + 10\ H^+ + 8\ e^-$$

The oxidation charge of the adsorbed Pt-S is assumed to correspond to the total oxidation of sulfur species and $6e^-$ are used in the reactions below.

$$Pt\text{-}S + 3\ H_2O \leftrightarrow SO_3 + 6\ H^+ + 6\ e^- + Pt$$

$$Pt\text{-}S + 4\ H_2O \leftrightarrow SO_4^{2-} + 8\ H^+ + 6\ e^- + Pt$$

Sulfurization of porous ZnO is usually performed at temperatures ranging from 150 to 450 °C. Sulfurization kinetics and the capacity of H_2S removal increases with an increase in temperature and it reaches maximum at 450 °C, followed by a reduction as the temperature continues to increase [48]. Sulfurization of ZnO by H_2S can be described by the steps shown in Figure 7:

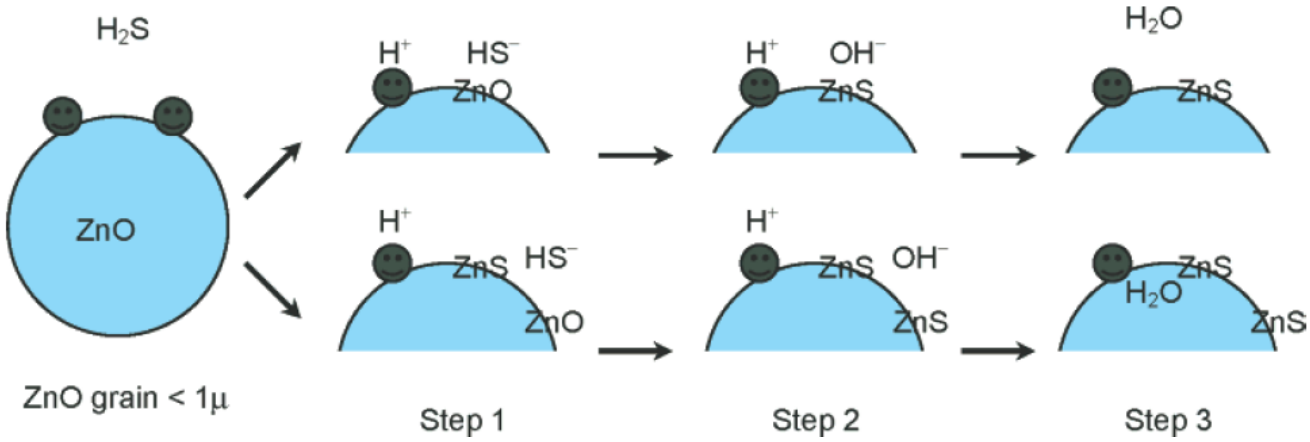

Figure 7. Sulfurization of ZnO with H_2S, including dissociation of H_2S, sulfurization of ZnO and neutralization of yielded OH^- from sulfurization and adsorbed H^+ form H_2O (as explained below) [48].

Step 1: H_2S molecule adsorbs and dissociates at the active sites on the solid surface. Depending on the surface structure and degree of sulfidation the active sites can be ZnO or ZnS.

$$H_2S + 2\bullet \rightleftharpoons H^+\bullet + HS^-\bullet$$

Step 2: Reaction between adsorbed HS^- and ZnO.

$$HS^-\bullet + ZnO = ZnS + OH^-\bullet$$

Step 3: Yielded OH^- and adsorbed H^+ form H_2O and active sites are reclaimed for the next cycle after water desorption.

$$OH^-\bullet + H^+\bullet = H_2O + 2\bullet$$

Ion migration was used to explain the sulfidation mechanism, as shown in Figure 8:

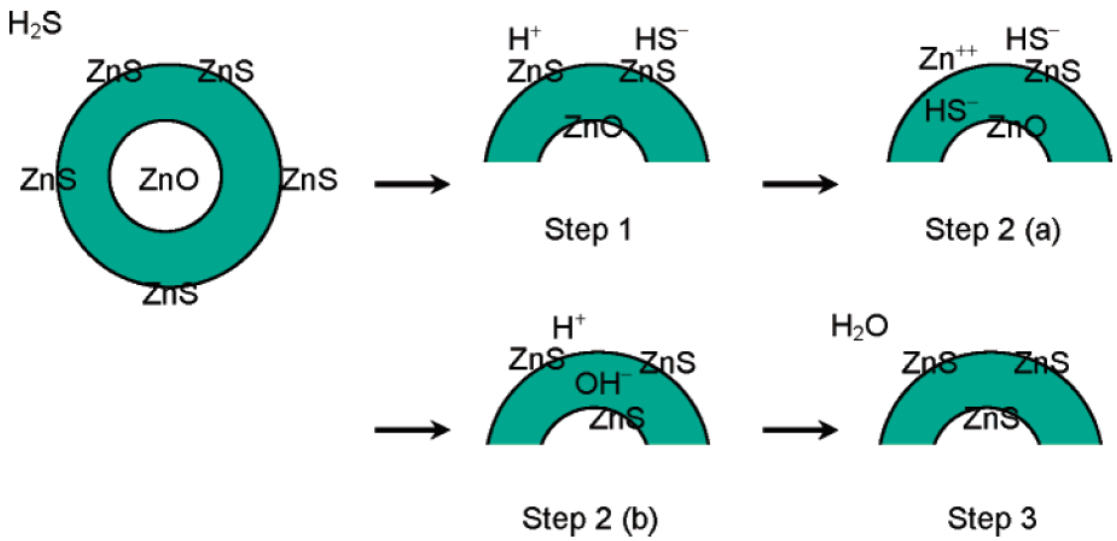

Figure 8. Ion migration and sulfidation penetration. HS^- ion penetrates the ZnS formed as external layer leading to the internal ZnO being sulfurized to ZnS [48].

Step 1: H_2S adsorbs on two active sites of ZnS on a completely sulfided grain surface.

$$H_2S + 2\bullet \rightleftharpoons H^+\bullet + HS^-\bullet$$

Step 2a: H^+ reacts with ZnS and forms HS^-.

$$H^+\bullet\ (ZnS) = Zn^{2+}\bullet + HS^-$$

The formed HS^- migrates to the boundary of ZnS and reacts with ZnO.

$$HS^- + ZnO = ZnS + OH^-$$

The formed OH^- migrates and combines with the adsorbed H^+ formed in Step 2b.

Step 2b: The adsorbed HS^- on the surface combines with Zn^{2+} left by proton dissociated.

$$HS^-\bullet + Zn^{2+}\bullet = ZnS + H^+\bullet + \bullet$$

The sulfidation of the second layer of ZnO is in process.

Step 3, The formed OH^- in Step 2a migrates and combines with the adsorbed H^+ formed in Step 2b and active sites are liberated through water desorption.

$$OH^-\bullet + H^+\bullet = H_2O + 2\bullet$$

2.5 SUMMARY

Catalytic desulfurization is essential for advanced industrial processes to fully take advantage of all outputs from processing fuel feedstocks as well as to prevent deleterious consequences of nonaction. Technology currently used to adsorb and oxidize hydrogen sulfide in these gas streams include using activated carbon as a highly effective sorbent and as a support for desulfurization catalyst metals including copper, iron, zinc, and palladium. ACFs have significant capacity for hydrogen sulfide uptake but are not used as extensively as activated carbons. It has been shown that hydrogen sulfide adsorbs onto the ACF surface and is oxidized to elemental sulfur or sulfur compounds, including COS, SO_2, CS_2 or SO_4^{2-}. To the best of our knowledge, the mechanism and role of active surface chemistries on ACF surfaces in the elimination of H_2S is limited.

To clarify the quantity and nature of the functionalities on carbon surface is helpful to understand their effect on sulfurization. Boehm Titration is frequently used to investigate functionalities involving acid functional groups (CHO, COOH) and basic functional groups, as many oxygen functional groups exist in tremendously varied quantities on the surface of different carbons. Further, determining and quantifying carbon surface functional groups aids in interpreting the reaction between hydrogen sulfide and carbon surface. The effect of temperature on H_2S uptake by carbons is critical in the application of syngas clean-up.

Lanthanum and Ce (III) oxides have excellent sulfidation thermodynamics in realistic reformate gas compositions, especially the ones produced by steam reforming, autothermal reforming, or by coal gasification. Although these rare earth metal oxides have potential to remove sulfur and are able to be regenerated, the capacity of sulfur uptake is still far behind the other well developed metal sorbents such ZnO, CuO-Cr_2O_3, and others. In terms of regeneration,

it is not practical to regenerate spent sorbents by taking sorbents out of the reactor, dissolving formed elemental sulfur with carbon disulfide (CS_2) solvent, washing away formed sulfate on the sorbents with water and finally putting the sorbents back to the reactor after being dried.

In this work we use metal and impurity free activated carbon fibers (ACFs) as an evaluation platform to determine the most important parameters for optimal desulfurization of syngases. By changing the surface chemistry of the ACFs, the species responsible for sorption and catalysis can be unambiguously determined. We compare the functional groups (especially acidic and basic) typically observed on carbon black, graphite and ACFs to their role in desulfurizing simulated syngas over the temperature range of 110 to 170 °C. To develop and improve the potential of H_2S removal by rare earth metal, in this study, cerium and lanthanum oxides were used to remove H_2S from simulated syngas respectively and lanthanum oxide as well as lanthanum chloride were combined with activated carbon fibers as sorbents to adsorb/oxidize H_2S.

3.0 MATERIALS AND METHODS

3.1 MATERIALS

3.1.1 Materials

Carbon black Black Pearls 460 (BP460), Black Pearls 800 (BP800, Cabot Corporation, Massachusetts), Graphite (Alfa Aesar, Massachusetts) and activated carbon fibers, including ACF7, ACF10, and ACF15 (International Interchange Ltd., Michigan) were used in our research. Black Pearls and graphite were used as received, whereas activated carbon fibers were ground to powders and then passed through a 80 mesh sieve with a 177 μm opening. Cerium (IV) oxide (Sigma-Aldrich, St. Louis, Missouri), lanthanum oxide (Sigma-Aldrich, St. Louis, Missouri), lanthanum chloride $LaCl_3 \cdot 6H_2O$ (Fisher, Fair Lawn, New Jersey) and sodium hydroxide (Fisher, Fair Lawn, New Jersey) were used to impregnated activated carbon fibers ACF10 (International Interchange Ltd., Michigan). The average particle sizes of La_2O_3 and CeO_2 as measured by laser particle size analysis Microtrac S3500 (Microtrac Inc., Montgomeryville, Pennsylvania) are ~3.04 (Figure 9) and ~2.41 μm (Figure 28).

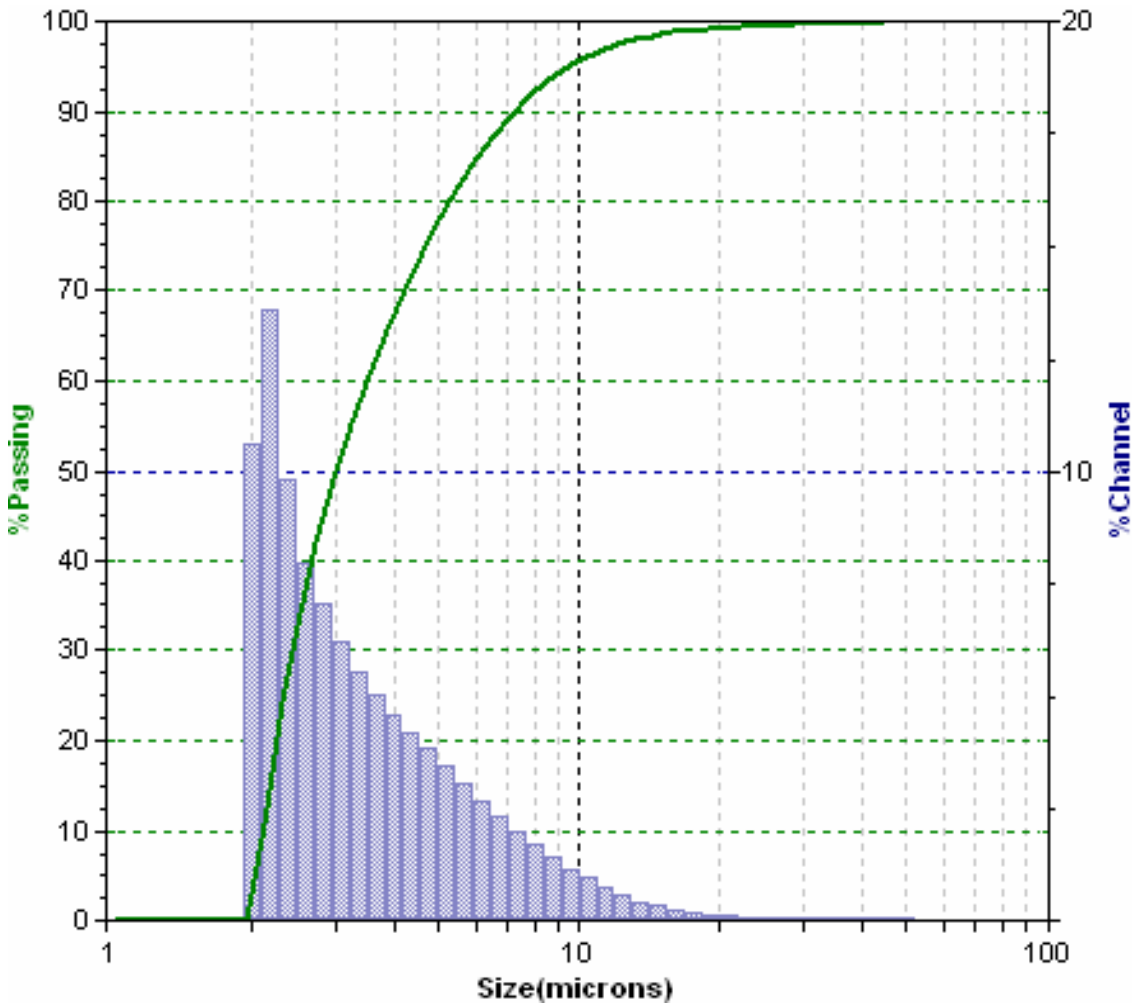

Figure 9. Particle size and distribution of La_2O_3 (2.1-68 μm), with an average particle diameter about 3.04 μm.

3.1.2 Simulated Syngas

Simulated syngas was formulated by mixing ultra high pure (UHP) grade H_2, N_2, CO, CO_2, O_2 and 5% H_2S (balance Ar). The syngas was based on the composition of syngas used at NETL (Table 2) and was believed to be representative of syngas for future power generation plants, as shown in Table 3.

Table 3. Composition of simulated syngas under dry and wet condition in this research, according to the syngas composition in NETL [16].

Gas	H_2	O_2	N_2	CO	CO_2	H_2S	Ar	H_2O	Total
Dry, %	24.4	0.4	17.4	34.6	15.2	0.4	7.6	0	100
Wet, %	24.4	0.4	16.8	34.6	15.2	0.4	7.6	0.6	100

3.2 EXPERIMENTAL SETUP AND SAMPLE PREPARATION

3.2.1 Experimental Setup

The catalytic material was placed into a fixed bed with a depth of 2 cm. This was done to maintain a constant space velocity. Typical amounts of material used varied based on the density of the material, ranging from 2.0 g for ACF to 12 g for graphite. The fixed-bed was supported by a coarse size frit at the bottom of the reactor. The reactor was positioned in the middle of a tube furnace (Model 55035, Lindberg, Riverside, Michigan). Mass flow controllers (Aalborg and MKS, Orangeburg, New York and Andover, Massachusetts) were utilized to adjust the flow rate of each gas such that the total flow rate was 0.5 L/min and the space velocity was 3800 hr^{-1}. The initial concentration of H_2S in the simulated syngas was 4000 ppm. To achieve 0.6% wet gas conditions, a portion of the nitrogen flow was directed to the water vapor generator, as shown in Figure 10. The sulfur content of the tail-gas was measured continuously by a residual gas analyzer (RGA, QMS300, Stanford Research Systems), through capillary column attached to a port on the outlet of the reactor. RGA calibration for H_2S was performed prior to and after syngas application.

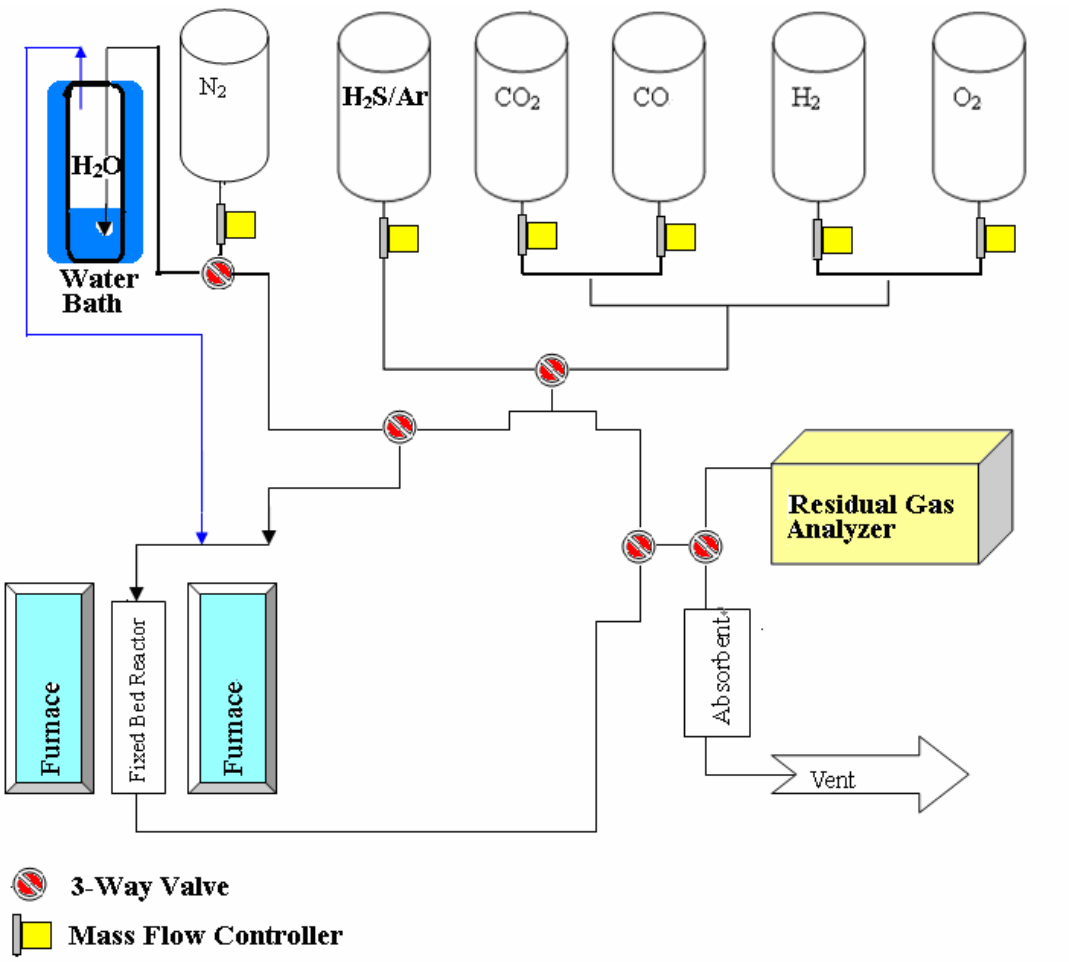

Figure 10. Schematic of carbon sorbents breakthrough capacity test. Syngas was simulated by mixing ultra high pure (UHP) gases. When water vapor was needed, N_2 was switched to water vapor generator to bring water vapor into gas mixture. Mass flow controllers (MFC) were used to adjust flow rate and making a total flow rate 0.5 L/min. For sulfurization, gas mixture was introduced into the fixed-bed reactor where catalyst was positioned and the tail gases through the catalyst were continuously monitored by the residual gas analyzer whose response time to the change of gas composition is less than 0.5 s. For regeneration of catalyst, N_2 was introduced into the reactor and remove absorbed sulfur species and the tail gases were also analyzed continuously by the residual gas analyzer.

3.2.2 Impregnation of Activated Carbon Fibers with Lanthanum Compounds

Wet impregnation was used as the main method to modify ACF sorbents according to the following procedures: 1) ACF-$LaCl_3$ was prepared by mixing 2.0 g ACF10 with 100 mL aqueous solution containing 2.0 g $LaCl_3$ for 4 hours and then dried in an oven at 140 °C overnight; 2) ACF-La_2O_3-NaOH was prepared by dissolving 0.31 mg La_2O_3 in 5 mL NaOH solution (1 M) in a sonicated solution and diluting with 100 mL DI water and subsequently mixing with 2.0 g of ACF. This solution was dried in an oven at 140 °C overnight; 3) ACF-$LaCl_3$-NaOH was prepared by mixing 2.0 g of ACF in $LaCl_3$ solution and titrating 102 mL of NaOH solution (0.25 M). This mixture was stirred for 4 hours by a stirrer and afterwards it was dried in an oven at 140 °C overnight.

3.3 SURFACE FUNCTIONALITIES ON CARBONACEOUS MATERIALS

Boehm titration is widely used to quantify the surface functional groups on carbonaceous materials [24]. Acidic sites were quantified under the assumption that NaOH neutralizes carboxyl, phenolic and lactonic groups; Na_2CO_3 carboxyl and lactonic; and $NaHCO_3$ only carboxyl groups.

Boehm titration was conducted according to the methods described by Boehm [49-51]. Briefly, standard acidic and basic solutions: 0.05N $NaHCO_3$, Na_2CO_3, HCl, NaOH, and 0.25N NaOH were prepared and HCl solution was used to standardize the other solutions via back titration. 2.0 g of each carbon sample was mixed with 100 mL of basic or acid solution and shaken for 24 hours. After that, carbon samples were separated by filtration and the remaining

basicity was determined by titration with 0.05N HCl while the remaining acidity was determined by titration with 0.05N NaOH.

3.4 SULFURIZATION AND REGENERATION EXPERIMENT

Simulated syngas was dosed to 2.0 g of each carbon sorbent in a down-flow fixed bed quartz reactor at temperatures ranging from 25 to 210 °C. The inlet concentration of H_2S was tested by RGA before sorbent sulfurization by sending the simulated syngas directly to the capillary via a bypass channel. For sulfurization, the gas mixture was switched to the fixed bed reactor and the effluent H_2S concentration was monitored with time. The experiment was shifted to the regeneration cycle when the outlet concentration of H_2S was equal to the inlet concentration, by venting the syngas and exposing the carbon to N_2. In this fashion we characterized desorption of sulfur species, regeneration, and subsequent sulfurization and regeneration

Regeneration temperature was 400 °C after sulfurization ranging at the temperature of 110 °C or 170 °C. When total breakthrough was reached, influent gas was switched from simulated syngas to N_2 only and temperature increased to 400 °C for the regeneration cycle. After regeneration was finished, temperature was decreased to sulfurization temperature and syngas was introduced again. Each sorbent was treated for three cycles.

3.5 THERMOGRAVIMETRIC ANALYSIS

Thermal gravimetric analysis (TGA 7 - Perkin Elmer, Waltham, Massachusetts) was performed on select sulfurized carbon samples by heating from room temperature to 600 °C at different scan rate (2, 5, 10, 20 or 40 °C/min) . Based on the Arrhenius equation Ea = - R T ln (k/A), plotting of the logarithm of the scanning rate versus the inverse of the absolute temperature can be used to determine activation energy of desorption of sulfur species [52].

4.0 RESULTS AND DISCUSSION

4.1 H_2S UPTAKE ONTO CARBONACEOUS SORBENTS

4.1.1 Functional Groups on Carbon Surface

Boehm Titration of carbonaceous materials was performed to quantify basic and acid functional groups on carbon surface. It was determined that acidic functional groups are the dominating functionalities on carbon black and graphite surface, whereas basic functional groups are more pronounced functionalities on activated carbon fibers surface as shown in Table 4. Carbon black samples were found to have elevated levels of acid functional groups (carbonyl and carboxyl groups, Table 10, Appendix) compared to other carbon materials tested, which is typical of carbon blacks [49]. These acidic groups dominate the surfaces of carbon black because of the production process while the carbon feedstock was heated with oxygen below its ignition temperature, producing surface oxides with acidic properties [50]. For activated carbon samples, during the activation process of carbon, carbon is heated and surface compounds are removed. When cooling to room temperature in vacuum or in an inert gas, carbon can bind oxygen and form basic surface oxides [50]. Further, the proportion of basic functional groups on carbon black is not as high as on other carbons such as activated carbon [53] or activated carbon fiber [43] because of manufacturing process highlighted above.

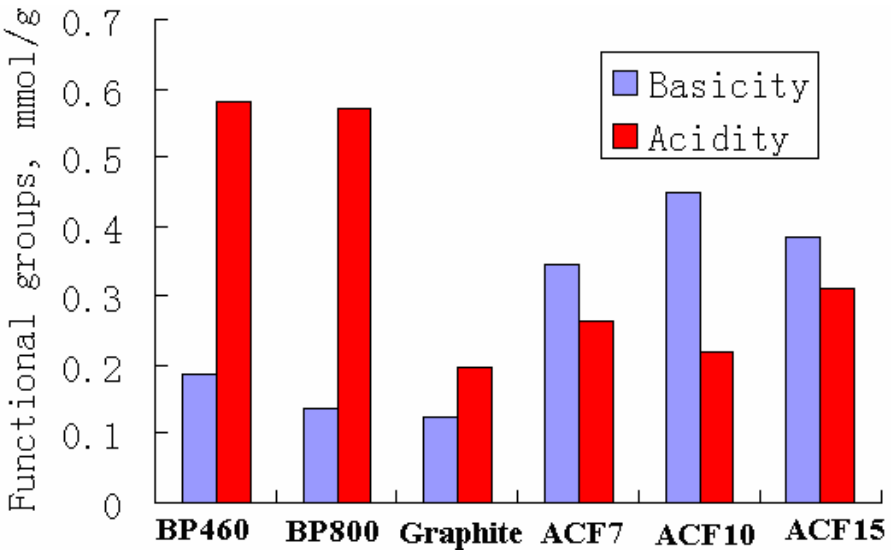

Figure 11. Basic and acid functional groups on carbon surface, determined by Boehm titration. Standardized HCl (0.05 N) was used to neutralize basic functional groups on the carbon surface and then standardized NaOH (0.05 N) was used to determine the residual amount of HCl so that the amount of HCl consumed by basic functional groups could be calculated. The amount of acid functional groups on carbon surface could be determined, vice versa. The most basicity 0.451 mmol/g and least acidity 0.217 mmol/g were found on ACF-10. The sum of total acidity and basicity groups of ACF7, ACF10 and ACF15 are 0.610 mmol/g, 0.670 mmol/g and 0.694 mmol/g respectively. There are more acidic functional groups than basic ones on carbon black and graphite.

Table 4. Functionalities on the surface of carbon blacks, graphite and ACFs, determined by Boehm titration. ACF10 has the largest surface area and number of basicity.

Sorbent	BP460	BP800	Graphite	ACF7	ACF10	ACF15
Surface Area, m^2/g	74.1	225	0.507	570	1403	1294
Basicity, mmol/g	0.186	0.136	0.124	0.345	0.451	0.383
Acidity, mmol/g	0.58	0.57	0.195	0.265	0.217	0.311
Total functional groups, mmol/g	0.766	0.706	0.319	0.61	0.67	0.694
Basic / Total, %	24.4	19.2	38.9	56.6	67.5	55.1

Contrary to carbon blacks and graphite, basic groups were more pronounced on activated carbon fibers (Table 4). Basic groups on ACF7 and ACF15 account for about 55% of total functional groups while the proportion of basicity groups on ACF10 is 67.5%.

4.1.2 H_2S Uptake onto Carbonaceous Materials

A synthetic syngas mixture containing 4000 ppm H_2S was dosed to samples through a fixed bed reactor and the H_2S content of the tail gas was continuously monitored. For consistency of measurement, initial breakthrough is determined when H_2S is initially detected and 88% H_2S breakthrough (3500/4000) is considered to be a complete breakthrough as tested at the packed-bed outlet. Changing the major composition of the syngas (i.e., doubling oxygen content) had little effect on hydrogen sulfide removal efficiency whereas it was significantly increased by the presence of water vapor.

It was found that the time of initial H_2S breakthrough with carbon blacks and graphite was less than 1 minute and about 1.5 minutes, respectively as shown in Figure 12. While a high inlet concentration of H_2S may lead to fast breakthrough; it does not affect the H_2S uptake capacity, which is a more important parameter for H_2S removal. Fast breakthrough of H_2S was due to the high inlet concentration of H_2S [35] and small surface area of carbon black. Complete breakthrough was reached very fast using BP460, about 2 minutes. The time of 88% breakthrough of H_2S when using BP800 was about 7 minutes. The H_2S uptake capacity of BP800 is a little higher than that of BP460 and the initial breakthrough time is also slightly longer than that of BP460. Such behavior is due to the fact that BP800 has about 3 times larger surface area (225 m^2/g) than BP460. BP460 has slightly more basic functional groups but the surface area also plays a very important role in H_2S uptake.

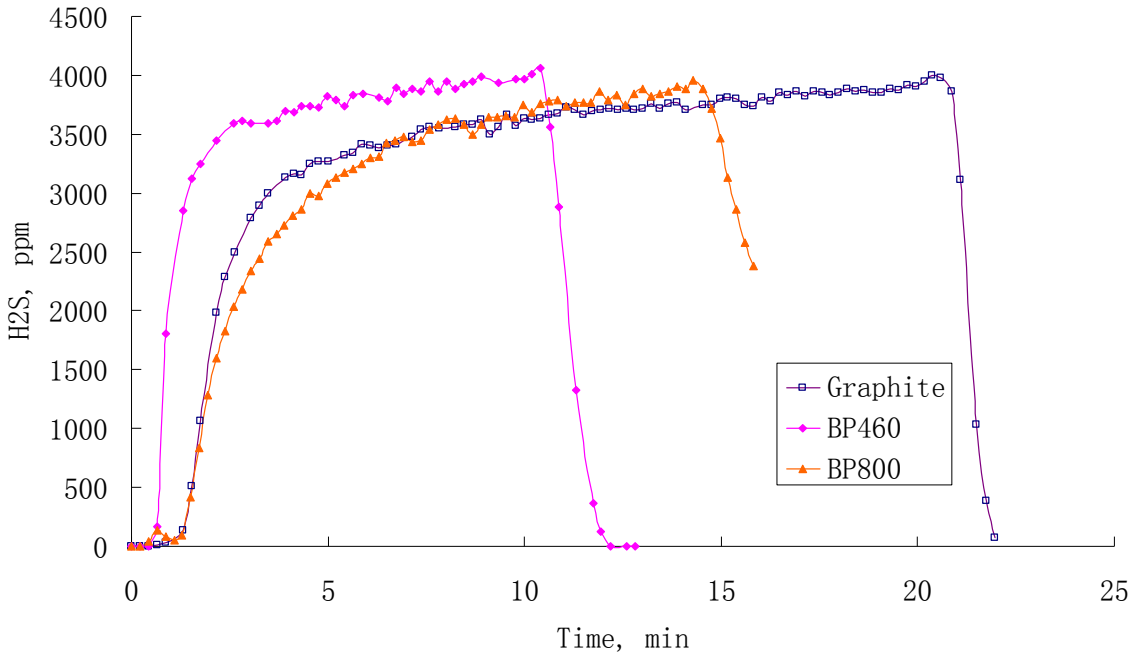

Figure 12. Breakthrough curves of 6 g of carbon black samples (BP460 and BP800) and 12 g of graphite. Sulfurization was performed at room temperature with 4000 ppm H_2S under dry condition. The total flow rate of simulated syngas was 0.5 L/min with a space velocity 3800 h^{-1}. When the effluent H_2S concentration reached 4000 ppm, inlet gas was switched to N_2 only. By integrating the area above each breakthrough curve, the H_2S-uptake capacity could be calculated. The capacity of BP460, BP800 and graphite is 1, 1.29 and 1.41 mg H_2S/g Sorbent, respectively.

Table 5. H_2S-uptake capabilities of carbon samples including carbon black (BP460 and BP800), graphite and activated carbon fibers (ACF7, ACF10 and ACF15). ACF10 has the highest capacity.

Carbon	BP460	BP800	Graphite	ACF 7	ACF 10	ACF 15
Initial Breakthrough Time, min	<1	1.5	1.5	3	3.5	4
88% Breakthrough Time, min	2	7	7.5	12	20	12
mgH_2S/g-Sorbent	1	1.29	1.41	6.74	10.2	7.58

Performance of ACF for H_2S uptake was much better than that of carbon black (6 mg H_2S/g Sorbent versus 1 mg H_2S/g Sorbent). This is believed to be due to the fact that more basic functional groups lead to higher adsorption of acidic H_2S by ACFs while abundance of acidic groups are the dominant functionalities on carbon black. Another reason for higher H_2S capacity is due to significantly larger surface area of ACF compared with carbon black. It is also observed that acidic groups on carbon black surface reduce H_2S uptake capacity because they prevent the dissociation of H_2S [54].

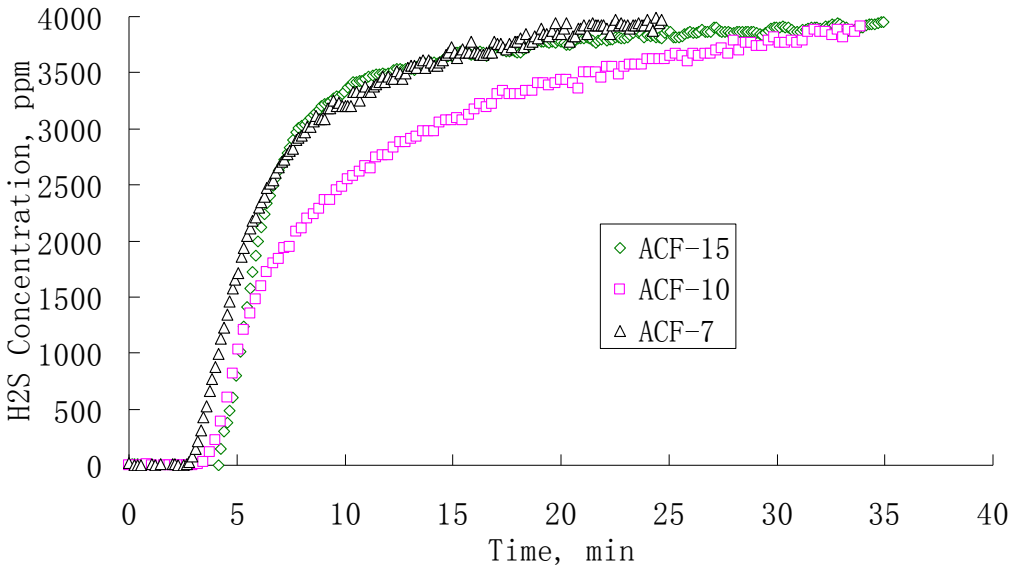

Figure 13. Breakthrough curves of ACFs. Sulfurization of 2.0 g ACF was performed with 4000 ppm H_2S at room temperature under dry condition. The total flow rate of simulated syngas was 0.5 L/min with a space velocity 3800 h^{-1}. By integrating the area above each breakthrough curve, the H_2S-uptake capacity could be calculated. The capacity of ACF-7, ACF-10 and ACF-15 is 6.74, 10.2 and 7.58 mg H_2S/g Sorbent, respectively.

For activated carbon fibers, the initial breakthrough time of H_2S range from 3 to 4 minutes. The initial breakthrough time with ACF7 is shorter than that with the other activated

carbon fibers. Such behavior can be explained by the fact that ACF7 has lower surface area compared to other fibers and less basic functional groups.

ACF10 has the highest H_2S-uptake capacity compared to other carbon sorbents because it has the highest surface area and strongest surface basicity. By integrating the area above the breakthrough curve on Figure 13, it is determined that 10.2 mg H_2S is adsorbed per gram ACF10. The capacity of ACF15 was 7.58 mg H_2S/g Sorbent because its basicity proportion of ACF15 is smaller than that of ACF10. Similar explanation is valid for ACF7.

4.2 EFFECT OF SURFACE FUNCTIONALITIES ON H_2S UPTAKE

The H_2S uptake capacity was determined to scale with the increase in basic functionalities for all materials tested, as shown in Figure 14. Our previous results showed that uptake of H_2S increased with the increase of density of basic functionalities on activated carbon fibers [55] and in this work it was determined that this is true for other carbon forms. The basic functional groups that exist on carbon surfaces are thought to have γ-pyrone-like structure [49], as shown in Figure 15. In the oxygen-containing aromatic rings, one of the electron pairs of the hetero-atoms contributes to the aromatic system with non-basicity, whereas the second lone pair extends in the plane of the ring forming basicity. Figure 16 shows the proposal reaction between basic functionalities and H_2S. Under wet condition, when water film forms on the carbon surface, dissociation of H_2S leads to formation of HS^-, which further reacts with basic sites. The basic aromatic rings are easily protonated to form aromatic cations and salts. The non-basic lone pair of electrons of the oxygen atom is delocalized and contributes to the aromatic π electron system.

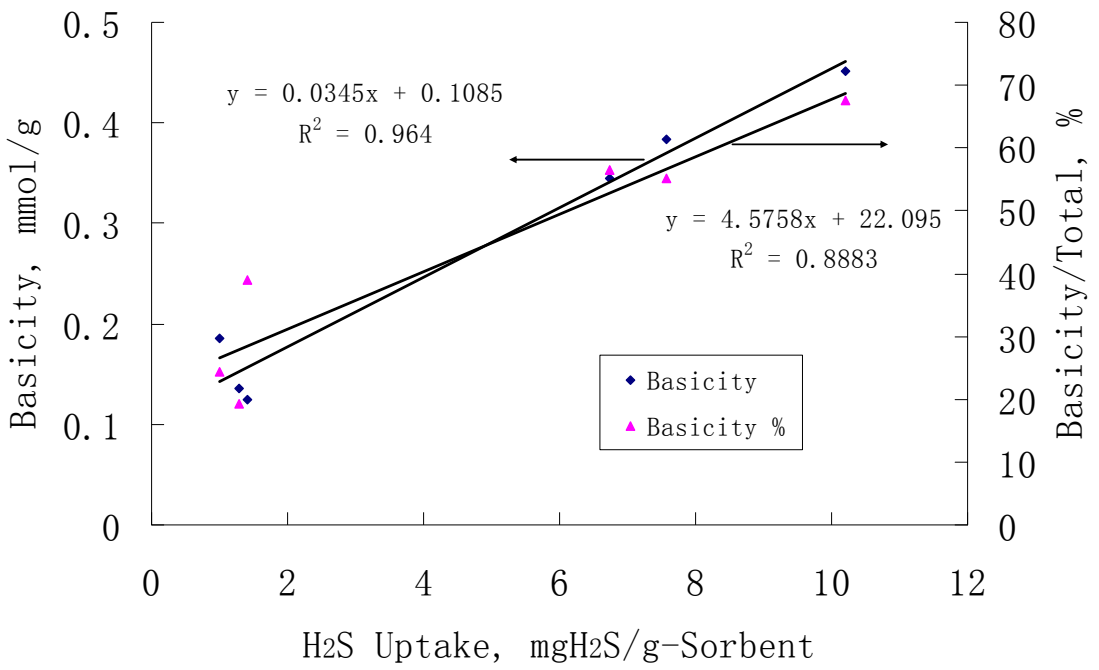

Figure 14. Relationship of capacity of H_2S uptake and basicity functionalities on the surface of carbon materials including carbon black (BP460 and BP800), graphite and activated carbon fibers (ACF7, ACF10 and ACF15). There is consistency between capacity and basicity, in terms of absolute amount or ratio. This consistency means that the more basic functional groups the higher H_2S-uptake capacity.

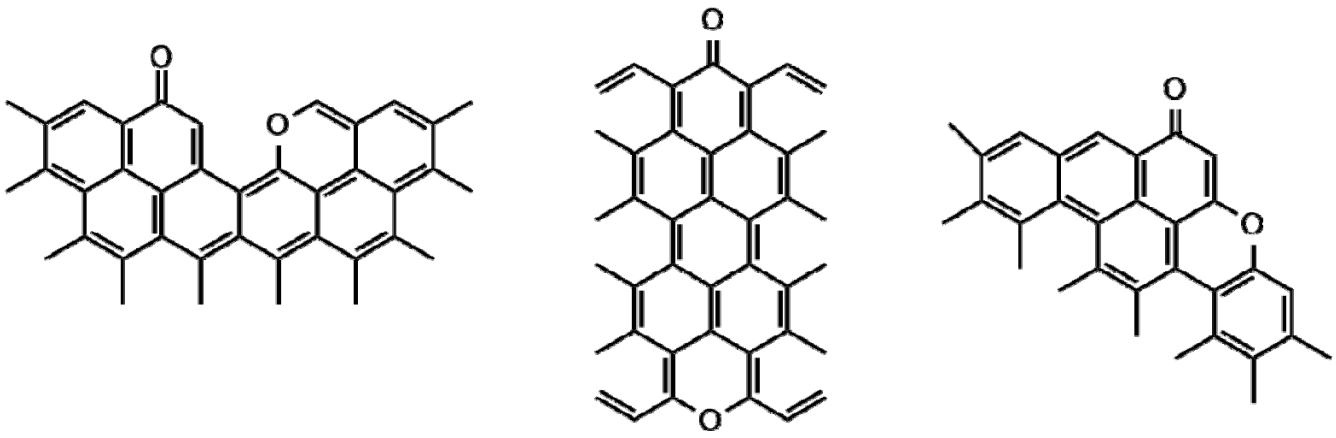

Figure 15. Possible basic surface sites on carbon surface having γ-pyrone-like structure, which has a ketone and an oxygen in a unsaturated six-member ring [49].

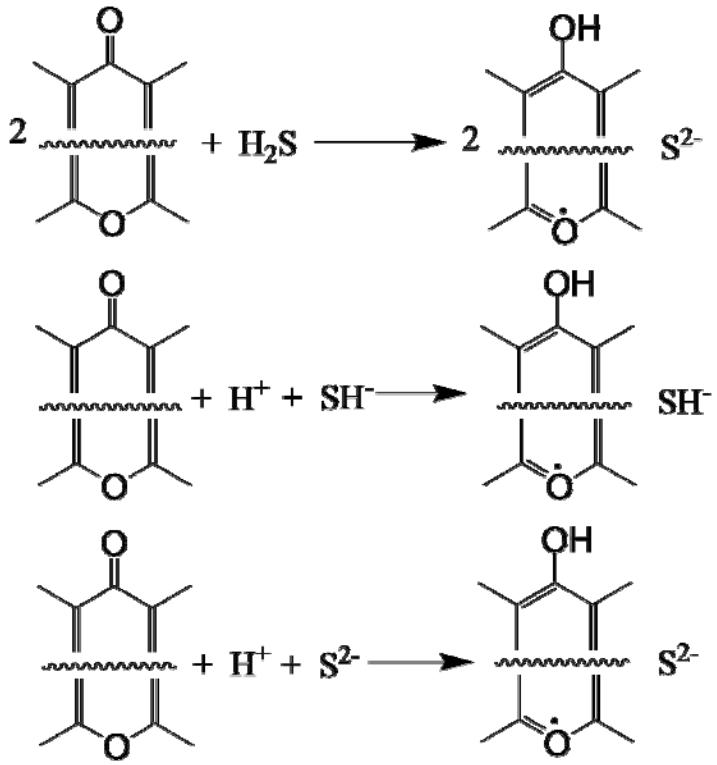

Figure 16. Proposed interaction between H_2S and basic sites on carbons surface under dry (upper one) and wet (middle and bottom ones) condition, adapted from [49]. Basic sites remove H_2S by the way that the ketone accepts a proton.

4.3 EFFECT OF WATER VAPOR ON H_2S UPTAKE

Sulfurization of carbon sorbents under wet condition was performed in the same fashion as under dry conditions with water added as described earlier. Table 6 presents data acquired at room temperature indicating H_2S-uptake capacity of ACF10 to be 18 mg H_2S/g Sorbent, approximately twice the capacity under dry condition. The higher capacity is due to oxidation of H_2S in the water film that is formed on activated carbon fiber surface under humid condition [56]. Flytzani-Stephanopoulos et al. [57] also found that low concentration of water could enhance the adsorption of sulfur. Furthermore, water plays an important role in the dissociation of H_2S and

favors the retention of H_2S which could be reflected by the longer initial breakthrough time as shown in Figure 17.

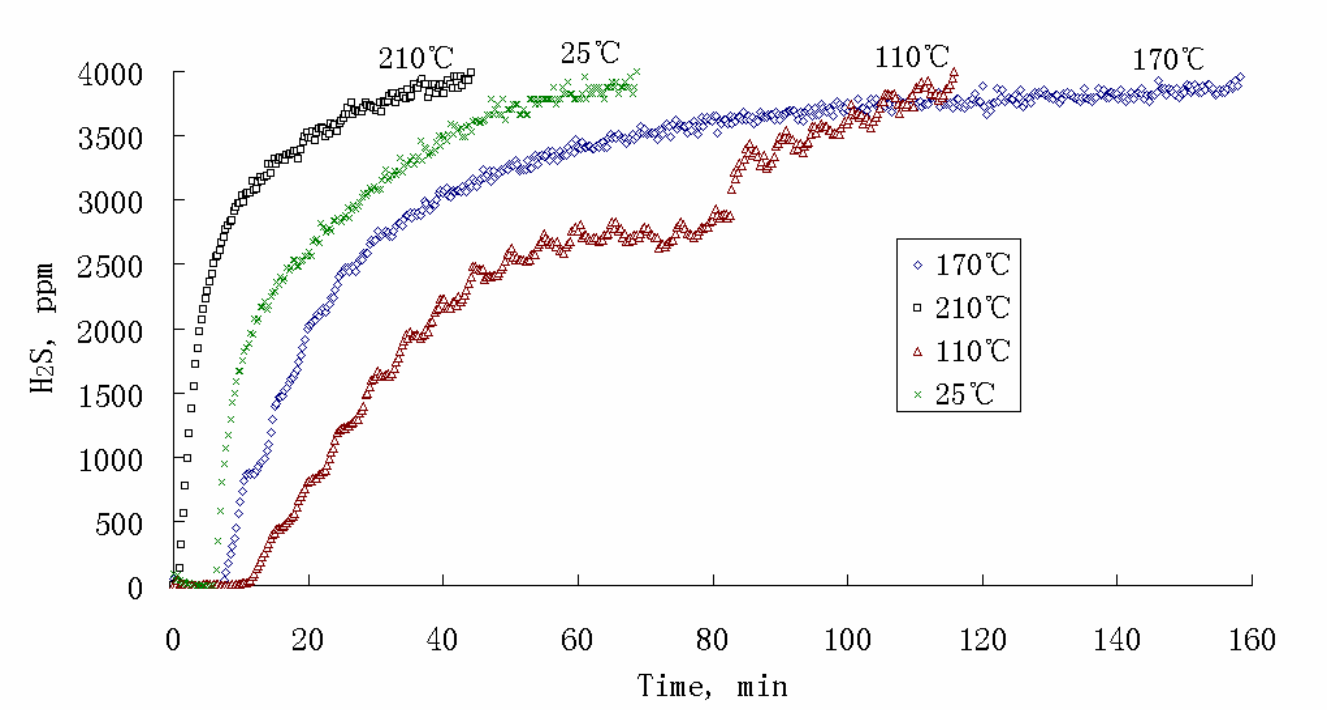

Figure 17. Sulfurization of 2.0 g ACF10 with 4000 ppm H_2S under wet condition at 25, 110, 170 and 210 °C respectively. The total flow rate of simulated syngas was 0.5 L/min with a space velocity 3800 h^{-1}. By integrating the area above each breakthrough curve, the H_2S-uptake capacity could be calculated.

Table 6. Breakthrough time and capacity of ACF10 under wet condition with 0.6% water vapor. The best H_2S-uptake capacity was obtained at the desulfurization temperature ranging from 110 to 170 °C.

Temperature, °C	**25**	**110**	**170**	**210**
Time of Initial Breakthrough, min	6	11	7.5	0.6
Time of 88% Breakthrough, min	37	45	60	19
Capacity, mg H_2S/g Sorbent	18	36	32	8
Capacity, mg H_2S/cm^3 Sorbent	2	3.3	3.6	0.89

4.4 TEMPERATURE EFFECT ON H_2S UPTAKE

4.4.1 Effect of Temperature on H_2S uptake

To understand the effect of temperature on H_2S uptake, ACF10 was sulfurized at 25, 110, 170 and 210 °C under wet conditions, the results of which are shown in Figure 17 and summarized in Table 6. It was determined that the maximum capacity, 36 mg H_2S/g Sorbent (Table 6), was obtained when sulfurization was performed at 110 °C. Desorption of each sulfurized sample was performed by thermal gravimetric analysis (TGA) at different scanning rates to obtain the activation energy of desorption, as shown in Figure 18. The activation energy of desorption of sulfur species from activated carbon fibers sulfurized at 25, 110, 170 and 210 °C are 34, 42, 40 and 89 kcal/mol respectively. The covalent bond energy of S-S, S-O and S=C are 54, 63 and 114 kcal/mol respectively [58]. In our sulfurization experiments, some or all of these bonds might form, possibly in the form of S_x, $SO_4^{2-}$and COS, respectively [3,56]. These interactions are more plausible than simple physisorption where the adsorption of H_2S to the surface occurs only through Van der Waals interactions, which require energy below 5 kcal/mol. Differences between the measured values and those of pure bonds listed above may be explained by the coupling of the measurement of the activation energy of the desorption (that is the average energy required for the desorption of physically adsorbed sulfur species) and the decomposition of some or all of the mentioned covalent bonds due to chemisorption.

The activation energies measured in this study are higher and more varied compared to desorption of sulfur species from platinum sorbent with activation energy of 27 kcal/mol [59]. However, this result was from the sulfurization experiment performed under extremely low temperature ranging from -123 ~ -188 °C. Bandosz et al. [24] found that significant weight loss

at the temperature ranging from 223~323 °C mainly attributes to elemental sulfur and physically desorption of H_2S should happen at lower temperature. Additionally, the surface of platinum is much 'cleaner' than that of ACF (with its various functional groups, thus leading to the formation of stronger covalent bonds such as S-O and S=C).

Sulfurization temperatures in the range from 110 to 170 °C (Figure 17) leads to the highest observed capacity for H_2S by all carbons tested. The uptake may be enhanced in this narrow temperature range because of an intricate balance between a thermal energy appropriate to form physical and chemical bonds between carbon and sulfur species and the presence of a water film in micropores of activated carbon fibers. When the temperature is under 100 °C or room temperature, water vapor may condense before it reaches the carbon bed so that it is not favorable to form water film on the carbon surface. On the other hand, the bonds between sulfur species and carbon are weaker because physical adsorption plays the main role at low temperature [60], as is seen in the activation energy of desorption at these temperatures. When the temperature is too high (e.g. 210 °C), water film is not as stable on the carbon surface. Such higher temperatures will also favor chemisorption over physical adsorption [60] and stronger chemisorption bonds formed at higher temperature are reflected by the higher activation energy of desorption. In addition, functionalities on carbon surface begin to decompose to CO_2 at 200 °C as shown in our previous results [55] where we showed that losing functionalities reduces the capability of activated carbon fiber to remove H_2S.

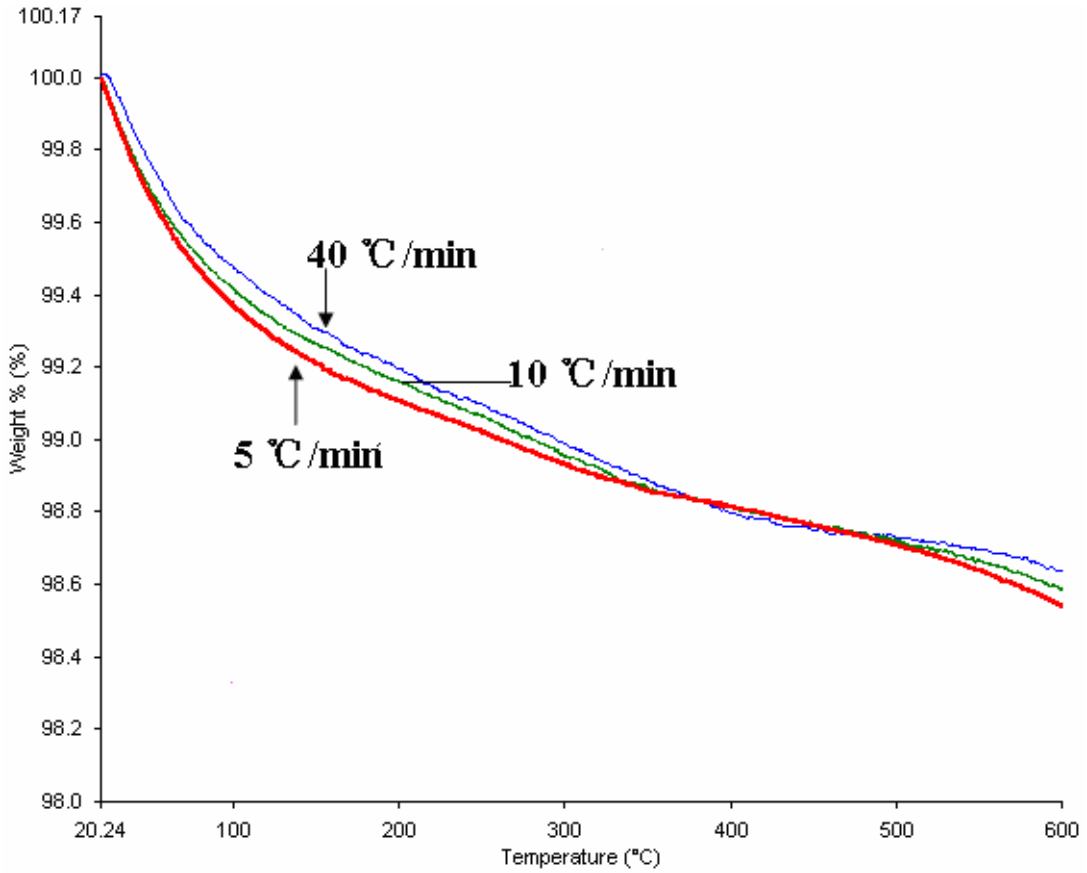

Figure 18. Activation energy of desorption analysis with TGA at different scan rate (5, 10 and 40 °C/min) using the activated carbon fiber sulfurized at 170 °C. The weight loss curve shifted at different scan rate. This data was analyzed and replotted as a Arrhenius plot in Figure 19 according to Arrhenius function.

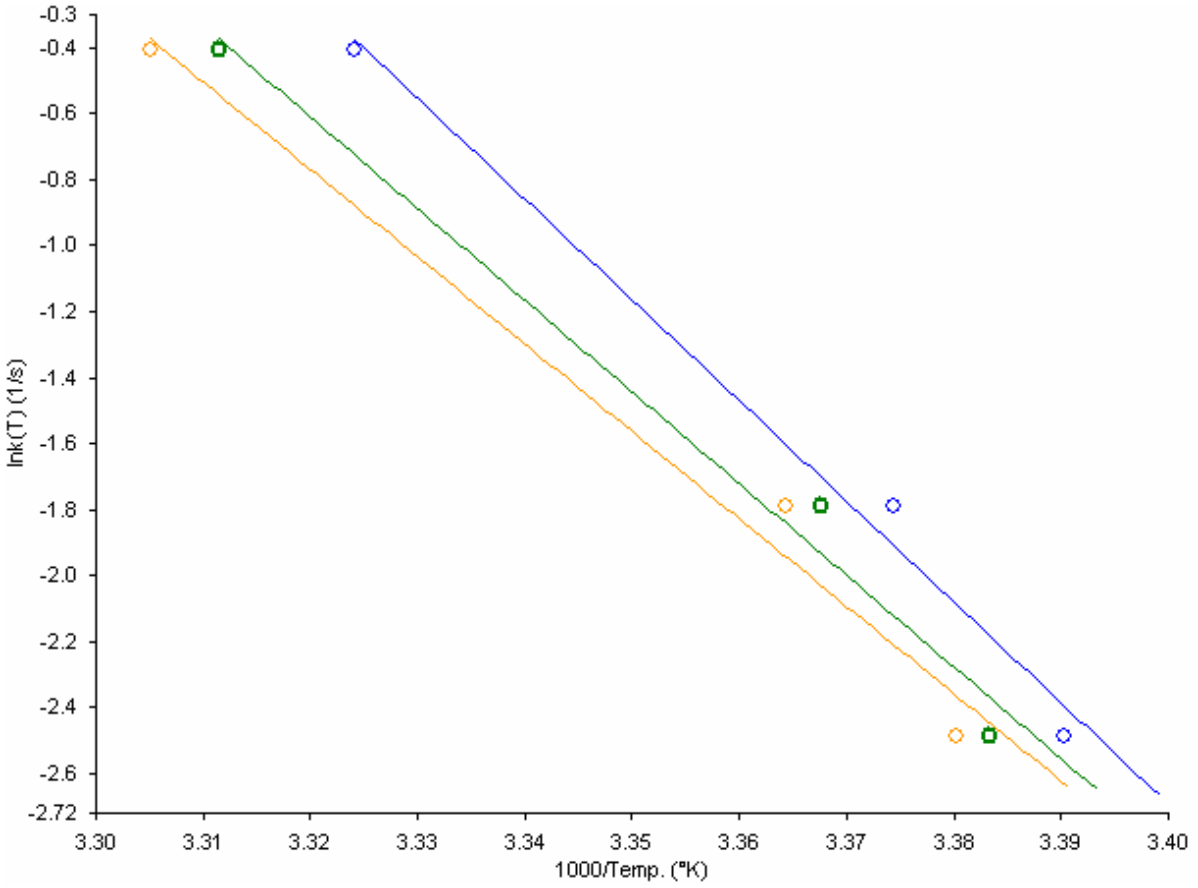

Figure 19. Arrhenius plot ln k vs. 1/T for the activation energy of desorption from slope using the activated carbon fiber sulfurized at 170 °C. k is the scan rate in terms of °C/s and upper three points from the TGA curve with scan rate 40 °C/min, middle three points from the TGA curve with scan rate 10 °C/min, and bottom three points from the TGA curve with scan rate 5 °C/min.

4.4.2 Effect of Heat Pretreatment at Different Temperature

The surface area of the activated carbon fibers after heat pretreatment decreased with the increase of treatment temperature, and meanwhile the pore width increased slightly, as shown in Table 7. Qiao et al. [61] also found that although high temperature treatment decreased the BET surface area, the micropore size is much more uniform with a more narrow distribution than those processed at lower temperature. While the surface area decreased with the increase of

heating temperature; an increase in pore width and decrease in micropore volume was observed [42]. Chiaki explained that removal of functional groups on carbon surface and gasification of part of the micropore wall creates wider pore width and that some micropores became closed pores for reconstructing micro-graphitic leading pore volume decreases.

Oxygen functionalities on carbon surface begin to decompose to CO_2 above 200 °C [55]. It is possible that more functional groups were lost at 500 °C compared with 300 °C and the surface area of the ACF treated at 500 °C is 9% smaller than that of original activated carbon fiber. ACF treated at a not high temperature (300 °C), had slightly smaller surface area than that of the ACF without treatment. It seems that heat treatment of ACF 300 °C is not so significant but the uptake of H_2S increased. When the outlet concentration of H_2S reaches 3500 ppm, the capability of H_2S uptake is very weak, as the desulfurization with the sample heat treated at 300 °C shown in Figure 20. When 3500 ppm of H_2S in the tail gas is considered as total breakthrough of H_2S (88% breakthrough), it can be noticed that the uptake amount of H_2S by ACF without heat treatment is bigger than that of ACF treated at 300 °C for 4 hours from Figure 20.

Table 7. Capacity of H_2S Uptake with ACF10 after heat pretreatment (300 and 500 °C) and fresh ACF. Pore width, volume, surface area and capacity of these samples are compared.

Pretreatment Temperature (°C)	Pore Width (nm)	Pore Volume (cm^3/g)	BET Surface Area (m^2/g)	H_2S Uptake mg H_2S/g Sorbent
500	3.18	0.131	1276	8.06
300	3.3	0.194	1344	12.6
Without Pretreatment	3.33	0.188	1403	10.2

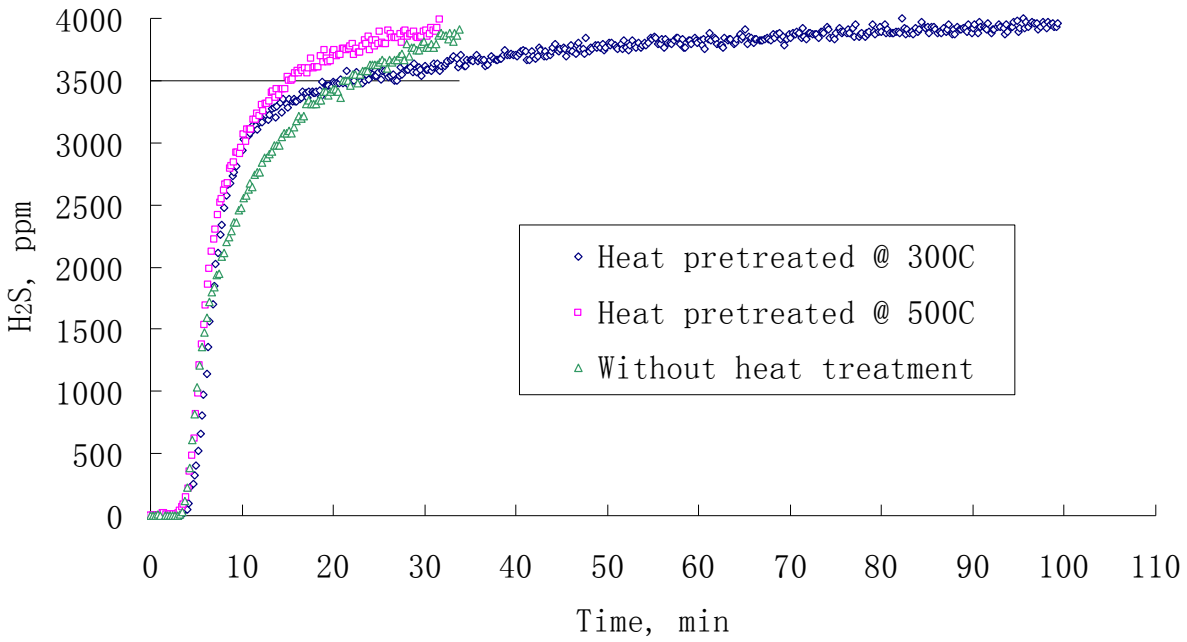

Figure 20. Breakthrough curve with ACF10 after heat pretreatment and fresh ACF. ACF10 was heated at 500 °C and 300 °C for 4 hours and sulfurized at room temperature with 4000 ppm H_2S under dry condition. The total flow rate of simulated syngas was 0.5 L/min with a space velocity 3800 h^{-1}. By integrating the area above each breakthrough curve, the H_2S-uptake capacity could be calculated.

Heat treatment of activated carbon fibers reduces surface area and pore volume and removes functionalities, leading to adverse effect on the capacity of H_2S uptake. Activated carbon fibers are different from metal oxides which are heated or calcinated under high temperature to create more active sites and surface area before being used to remove H_2S [28,57,62]. Calcination applied to metal oxide can bring about a thermal decomposition, phase transition, or removal of a volatile fraction; whereas for activated carbon fibers heat treatment removes functionalities on the surface including the basic functionalities that could enhance H_2S uptake.

4.5 REGENERATION OF SORBENTS

4.5.1 Sulfurization and Regeneration of Lanthanum Oxide and Cerium Oxide

Utilization of rare earth metal oxides, La_2O_3 and CeO_2, to remove H_2S was investigated for sulfurization at room temperature and the regeneration of these metal oxides was performed by switching simulated syngas to N_2 at 400 °C. It was found that the capacity of La_2O_3 in the 1st cycle was 2.33 mg H_2S/g Sorbent and that of CeO_2 was 0.758 mg H_2S/g Sorbent, as shown in Table 8. It is noticed that the surface area of sorbents before and after being sulfided was nearly the same, which demonstrates that the rare earth metal oxides have very good regenerative ability.

Table 8. Comparison of H_2S-uptake capacity, surface area before and after sulfurization of La_2O_3 and CeO_2 between this study and reference.

Sorbent	**La_2O_3**		**CeO_2**	
Result	**This study**	**Reference** [8]	**This study**	**Reference** [8]
H_2S Uptake, mg H_2S/g Sorbent	2.33	0.80~0.90	0.758	1.00 ~ 1.20
Surface area (Presulfided), m^2/g	4.86	3.5 ± 0.6	1.96	10.2 ± 0.4
Surface area (Sulfided), m^2/g	4.65	3.4 ± 0.5	2.26	9.8 ± 0.2

H_2S-uptake capacity is not only related to surface area of sorbent but also the space velocity (the ratio of flow rate of influent H_2S-containing gas mixture to volume of sorbents). During Flytzani-Stephanopoulos' experiment, La_2O_3 and CeO_2 sorbents were prepared by a urea

coprecipitation/gelation method from rare earth metal nitrate hydrate and then calcined [30]. Higher surface area materials were created after calcination in the light of CeO_2 (10.2 ± 0.4 m^2/g, compared to that of commercial product, 1.96 m^2/g) but the surface area of their prepared La_2O_3 was not as high as that of our commercial product (3.5 ± 0.6 m^2/g, compared to that of commercial product, 4.86 m^2/g). The H_2S-uptake capacity of their prepared CeO_2 and our commercial product are comparable though their surface area is 5 times of ours. The reason is attributed to their much higher space velocity (400,000 hr^{-1}) which is 100 times of ours, since such a high space velocity could lead to voids inside the pores when the mouths of pores are blocked by rapid accumulation of sulfur species, resulting in the decrease of H_2S-adsorption efficiency of pores. In the same way, when both La_2O_3 have approximate surface area, H_2S-uptake capacity of our commercial product is about 4 times of that of their prepared La_2O_3 due to the gradual adsorption of H_2S lessening the presence of voids.

The H_2S-uptake capacities of sorbents after regeneration are not as good as that of original sorbents due to the incapable removal of chemically adsorbed sulfur species. The H_2S-uptake capacity of La_2O_3 in the 2nd cycle is three times less than that in the 1st cycle (Figure 21) and in the 3rd cycle it is about 1/6 of that in the 1st cycle. That is because the regeneration was performed at room temperature with N_2 flow which could only remove physically adsorbed H_2S. The H_2S-uptake capacity of CeO_2 in the 2nd cycle is about 2/3 of that in the 1st cycle (Figure 22), and in the 3rd cycle it is just one third of that in the 2nd cycle. During the regeneration of CeO_2 after 1st sulfurization, a clear side peak appears (Figure 22), which is due to desorption of H_2S retained on the surface of CeO_2. Such behavior indicates that chemisorption of H_2S or its byproducts since the recovery of physically adsorbed species did not recover the original capacity.

Gas mixtures containing O_2 [27] or H_2 and H_2O [57] have been used to regenerate metal oxide sorbent. Regeneration performed at high temperature up to 800 °C in an oxygen-contained atmosphere could continuously obtain high H_2S-uptake capacity [57]. Reaction functions of sulfurization and regeneration of metal oxide sorbents are shown below, where MO represents metal oxide and MS represents metal sulfide.

$$H_2S + MO \rightarrow MS + H_2O \qquad \text{(Sulfurization)}$$

$$2\ MS + O_2 \rightarrow 2\ MO + 2\ S \qquad \text{(Regeneration)}$$

Regardless of the gas used for regeneration, our regenerative adsorption of H_2S experiments show that the commercial La_2O_3 and CeO_2 also have the potential to be regenerated and in the later experiment, La-modified ACF sorbents were used to remove H_2S in order to obtain high H_2S removal efficiency as well as good regeneration capability.

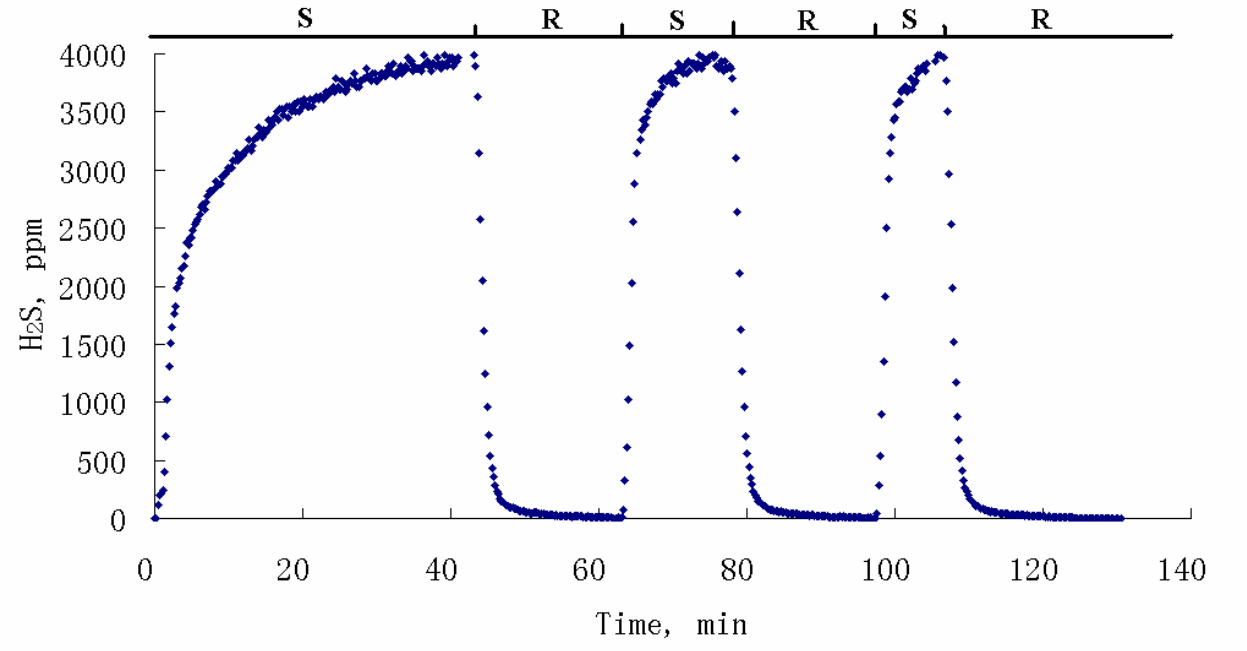

Figure 21. Sulfurization (S) and regeneration (R) of 6 g La_2O_3 for 3 cycles in order to test the regeneration capability. Sulfurization was performed at room temperature with 4000

ppm H_2S under dry condition. The total flow rate of simulated syngas was 0.5 L/min with a space velocity 3800 h^{-1}. When the effluent H_2S concentration was equal to 4000 ppm, syngas was switched to N_2 to begin regeneration. When the effluent H_2S concentration was equal to 0 ppm, N_2 was switched to syngas to begin another cycle of sulfurization and regeneration.

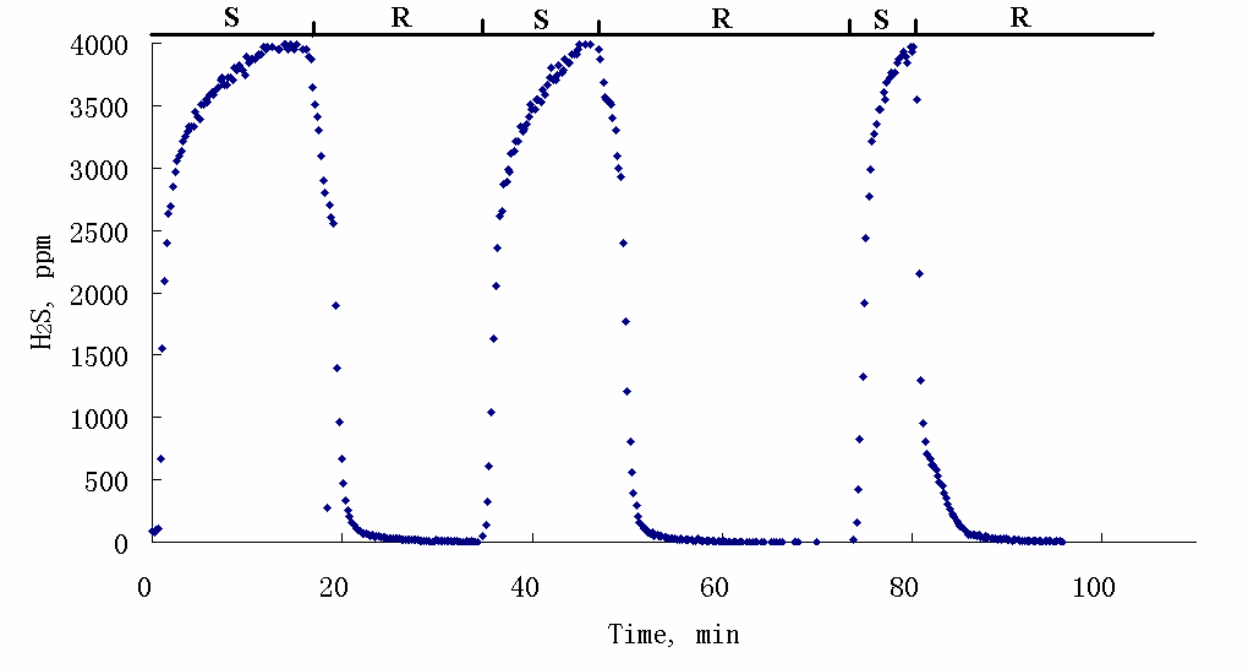

Figure 22. Sulfurization (S) and regeneration (R) of 6 g CeO_2 for 3 cycles in order to test the regeneration capability. Sulfurization was performed at room temperature with 4000 ppm H_2S under dry condition. The total flow rate of simulated syngas was 0.5 L/min with a space velocity 3800 h^{-1}. When the effluent H_2S concentration was equal to 4000 ppm, syngas was switched to N_2 to begin regeneration. When the effluent H_2S concentration was equal to 0 ppm, N_2 was switched to syngas to begin another cycle of sulfurization and regeneration.

4.5.2 Sulfurization and Regeneration of ACF10

Fresh ACF samples were subjected to three cycles of sulfurization and subsequent regeneration. Table 9 summarizes the surface area of original ACF sample and samples after modification, initial and 88% breakthrough times and H_2S capacity in mg H_2S/g Sorbent and mg H_2S/cm^3-Sorbent for the three adsorption/regeneration cycles. Time of 88% breakthrough indicates the time when 3500 ppm of H_2S at the outlet could be detected, which is considered as total breakthrough. These results show that the surface area of ACFs decreases significantly because majority of pores were occupied by additive particles such as metal oxides, metal hydroxide or metal chloride.

Table 9. Experiment results of sulfurization and regeneration of various sorbents. Surface area of modified samples decreased significantly because of the occupation of pores on ACF surface by additive chemicals. H_2S-uptake capacity in the 1st cycle is much better than that in the 2nd and 3rd cycles because N_2 could only remove physisorption sulfur species during regeneration and partly recover the H_2S-uptake capacity.

Sample	**ACF**			**ACF-$LaCl_3$**			**ACF-La_2O_3-NaOH**			**ACF- $LaCl_3$-NaOH**		
Surface area, m^2/g	1403			347			-			522		
Cycle	1st	2nd	3rd	1st	2nd	3rd	1st	2nd	3rd	1st	2nd	3rd
Time to Initial Breakthrough, min	2.4	0	0	7	0	0	3	0	0	3	0	0
Time to 88% Breakthrough, min	42	9	9	40	26	36	89	5	11	68	18	12
Capacity, mg/g	20	6.3	6.8	11	5.9	7.9	35	5.5	6.5	14	3.4	3.1
Capacity, mg/cm^3	2.2	0.7	0.75	2.4	1.3	1.7	4.6	0.73	0.87	3.6	0.87	0.79

When utilizing virgin ACF10 as the sorbent, the initial H_2S breakthrough was reached a little faster in the 1st cycle, 2.4 minutes (compared to that with metal-modified sorbent samples, 3 ~ 7 minutes), but the amounts of byproducts SO_2 (< 100 ppm) and COS (< 300 ppm) were low (Figure 23). After sulfurization of the catalyst material, the inlet gas was switched from simulated syngas to N_2 only and the concentration of H_2S in the effluent gas decreased quickly. As the temperature increased (10 °C/min), a peak of H_2S appeared shortly after the regeneration began. This peak is ascribed to the desorption of H_2S retained on the surface of activated carbon fiber via physisorption. Physisorption relies on Van der Waals (weak intermolecular) interactions or intermolecular forces, so that physically adsorbed H_2S molecules detached easily from the ACF surface when they obtained sufficient energy in the period of increasing temperature (regeneration).

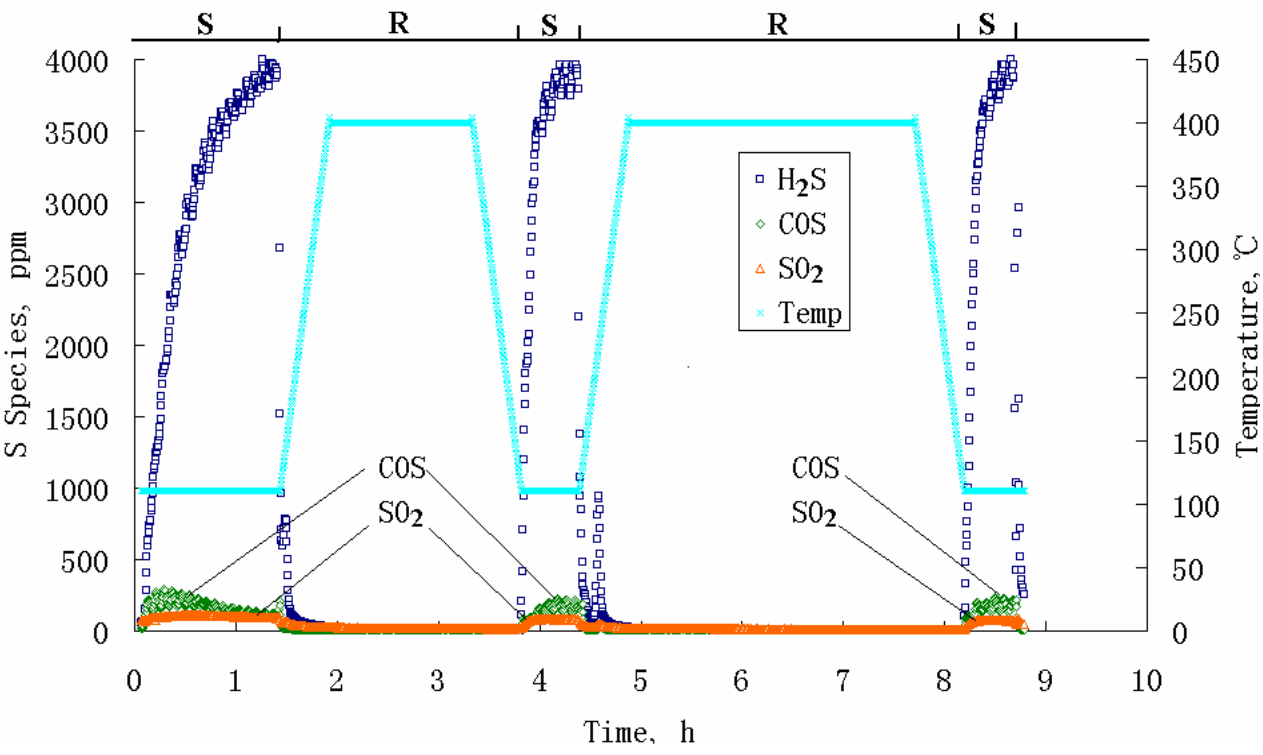

Figure 23. Sulfurization (S) and regeneration (R) of 2.0 g ACF10 under wet condition. Sulfurization with 4000 ppm H_2S at 110 ºC, when effluent H_2S concentration

reached 4000 ppm, simulated syngas was switched to N_2, and temperature was increased to 400 ºC for regeneration of sorbent for 2 to 3 hours. Then temperature was decreased to 110 ºC and another sulfurization and regeneration cycle began. By-produce including COS and SO_2 were also investigated.

The regeneration of ACF10 was inefficient because the capacity of H_2S uptake in the 2nd and 3rd cycle was about 1/3 of that in the 1st cycle. When the three-cycle experiment was finished and the reactor cooled down to room temperature with N_2 flush, some elemental sulfur was visibly observed to be adhered to the inside wall below the fixed bed as well as retained at the upper part above the carbon bed. The possible reasons affecting the poor ability for regeneration of ACF10 are as follows. The pores of the coarse-size glass frit of reactor (145 ~ 174 μm) which is used to support sorbents are plugged with additive metal compounds particles and ACF particles (~ 27 μm). Furthermore, elemental sulfur from ACF blocked the pores of the frit or formed a cake-like layer on top of the frit preventing other sulfur from leaving the reactor, since it was found that elemental sulfur remained on top of or inside the frit when sorbents were removed after experiment. That is why there was elemental sulfur remaining at the top of the reactor and possibly majority of sulfur still remained in the carbon bed.

4.5.3 Sulfurization and Regeneration of Lanthanum-Modified ACFs

Lanthanum compounds were selected to modify ACFs, since it was observed that the H_2S-uptake capacity of pure lanthanum oxide was much better than that of pure cerium oxide. The results of sulfurization and regeneration of ACF10 impregnated with $LaCl_3$ solution are shown in Figure 24. The surface area or the original sorbent decreased to a quarter of the initial surface area due to the fact that 84% of pores had been occupied by $LaCl_3$ precipitate, which could be reflected by

comparison of the pore volume of modified (0.03 m^3/g) and fresh (0.19 m^3/g) samples by BET experiment. In addition, $LaCl_3$ has strong water absorbability that would result in a certain amount of water being absorbed to further reduce the pore volume and surface area of sorbent under application conditions.

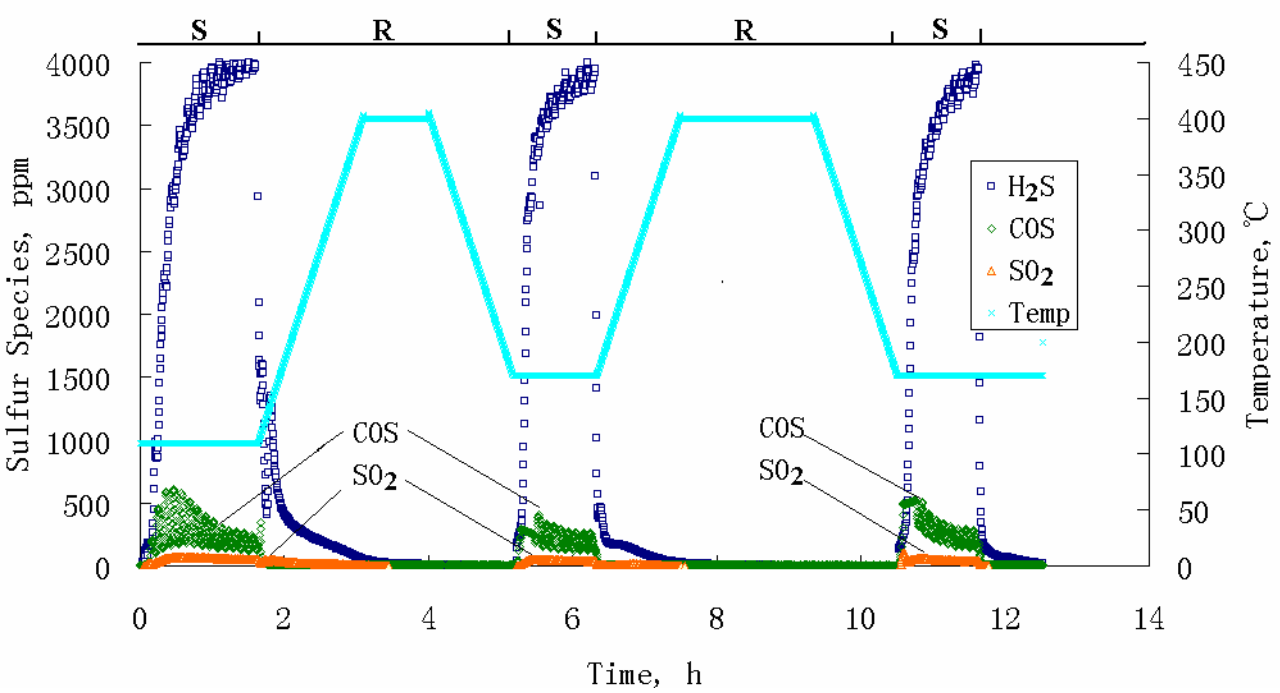

Figure 24. Sulfurization (S) and regeneration (R) of ACF-$LaCl_3$ under wet condition. Sulfurization with 4000 ppm H_2S, when effluent H_2S concentration reached 4000 ppm, simulated syngas was switched to N_2, and temperature was increased to 400 ºC for regeneration of sorbent. Then temperature was decreased to begin another sulfurization and regeneration cycle. By-produce including COS and SO_2 were also investigated.

Modified sorbent ACF10-$LaCl_3$ still had very good H_2S capacity in mg H_2S/cm^3-Sorbent (2.4 mg H_2S/cm^3 Sorbent) though its surface area was small (347 m^2/g, 25% of the original surface area). As the weight of the sorbent was nearly 4 g due to the addition of $LaCl_3$ but the volume was still the same as that of ACF10 only. The good behavior of H_2S removal (2.4

mg H_2S/cm^3 Sorbent) is ascribed to the strong water absorbability of $LaCl_3$ because more water was maintained on the surface on ACF10 forming water film, which could adsorb H_2S and aid the dissociation of H_2S. It was found that yellow elemental sulfur and black metal sulfide having metal brightness formed on the wall of the reactor. Possible reaction mechanisms related to the generation of metal sulfide and elemental sulfur on the surface of ACF are as follows:

$$LaCl_3 \rightleftharpoons La^{3+} + 3\ Cl^-$$

$$H_2S \rightleftharpoons H^+ + HS^-$$

$$3HS^- + 2\ La^{3+} \rightleftharpoons La_2S_3 + 3\ H^+$$

$$x\ H_2S + x/2\ O_2 \rightleftharpoons S_x + x\ H_2O$$

The capacity of H_2S uptake in the 2nd and 3rd cycles was less than that in the 1st cycle for ACF-$LaCl_3$, which means that the regeneration of the sorbent was still limited. During the sulfurization process in the 1st cycle, the pores might be saturated by water which could dissociate H_2S but also limit H_2S adsorption due to competitive adsorption. In the regeneration with N_2 flow at high temperature (400 °C), water accumulated in the pores and physically adsorbed H_2S were removed and pores were recreated. However a lot of pores were still occupied by salts, including metal chloride and metal sulfide. In the 1st cycle regeneration/desorption, one side peak appeared, presumably due to desorption of physically adsorbed H_2S. However, there was no observable side peak in the 2nd or 3rd cycle regeneration possibly because more metal sulfide was formed in the sulfurization of these cycles, thereby occupying more pores and reducing physisorption of H_2S.

The sulfurization and regeneration of ACF-La_2O_3-NaOH is shown in Figure 25. In the 1st cycle the capacity of H_2S uptake was as high as 35 mg H_2S/g Sorbent (or 4.6 mg H_2S/cm^3

Sorbent) but in the 2nd and 3rd cycles, the H_2S-uptake capacity was only about 15% of that in the 1st cycle. Possible reactions on the surface of this sorbent are listed below [26]:

$$NaOH + H_2S \rightarrow NaHS + H_2O$$

$$2\ NaOH + H_2S \rightarrow Na_2S + 2\ H_2O$$

$$La_2O_3 + 3\ H_2S \rightarrow La_2S_3 + 3\ H_2O$$

$$O_2 + 2\ H_2S \rightarrow 2\ S + 2\ H_2O$$

Since N_2 was used during regeneration at high temperature, it was not possible to oxidize metal sulfide to metal oxide. That is why the uptake capacity of H_2S in the 2nd and 3rd cycles was far behind that of the 1st cycle.

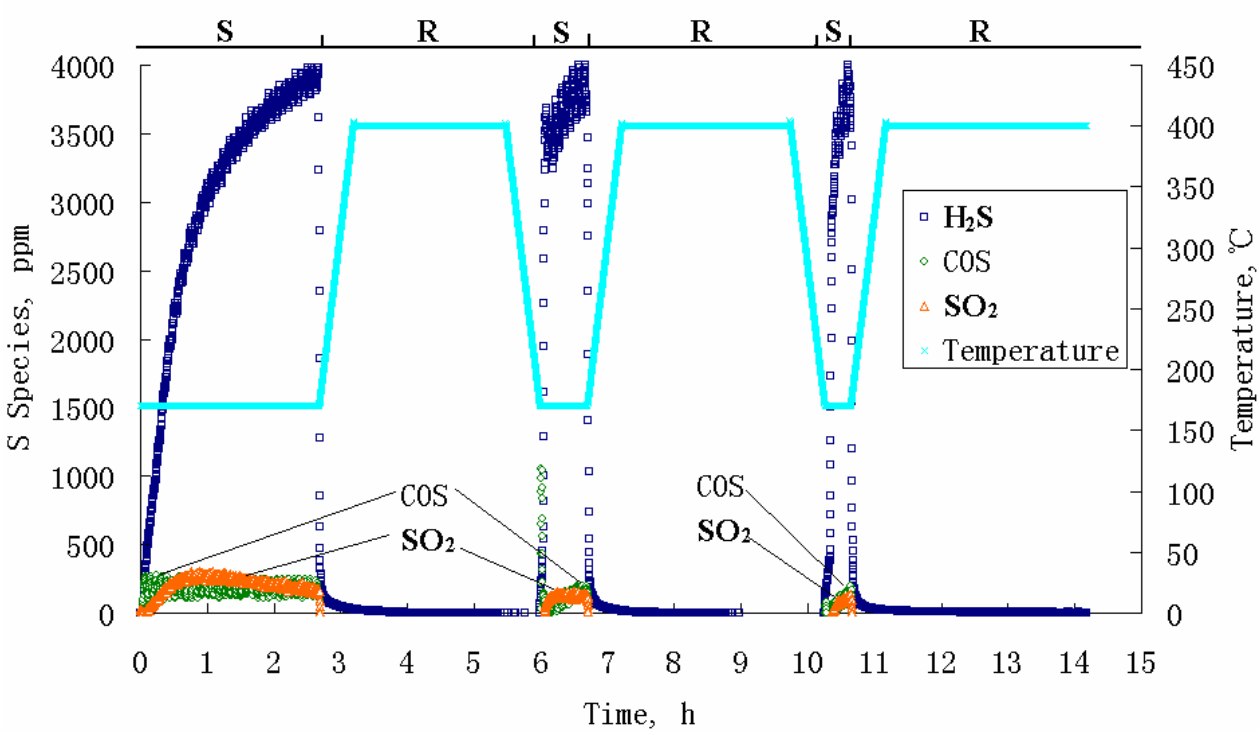

Figure 25. Sulfurization (S) and regeneration (R) of ACF-La_2O_3-NaOH under wet condition. Sulfurization with 4000 ppm H_2S at 170 ºC, when effluent H_2S concentration reached 4000 ppm, simulated syngas was switched to N_2, and temperature was increased to 400 ºC for regeneration of sorbent. Then temperature was decreased to

170 ºC and another sulfurization and regeneration cycle began. By-produce including COS and SO_2 were also investigated.

$La(OH)_3$ was the dominant lanthanum compound in this sorbent and a main factor reducing the surface area of sorbent for ACF-$LaCl_3$-NaOH sorbent. It is important to note that when the NaOH solution was mixed with $LaCl_3$ solution during the preparation of ACF-La_2O_3-NaOH sorbent, small white particles (presumably $La(OH)_3$ precipitation) formed. As the whole ratio of $LaCl_3$ to NaOH was 1:3; after filtration and desiccation, $La(OH)_3$ was the main residuals in the sorbent.

$$LaCl_3 + 3\ NaOH \rightarrow La(OH)_3 \downarrow + 3\ NaCl$$

The surface area of sorbent was severely decreased to approximately 1/3 of the original surface area of ACF due to the occupation of pores on the surface by $La(OH)_3$ particles.

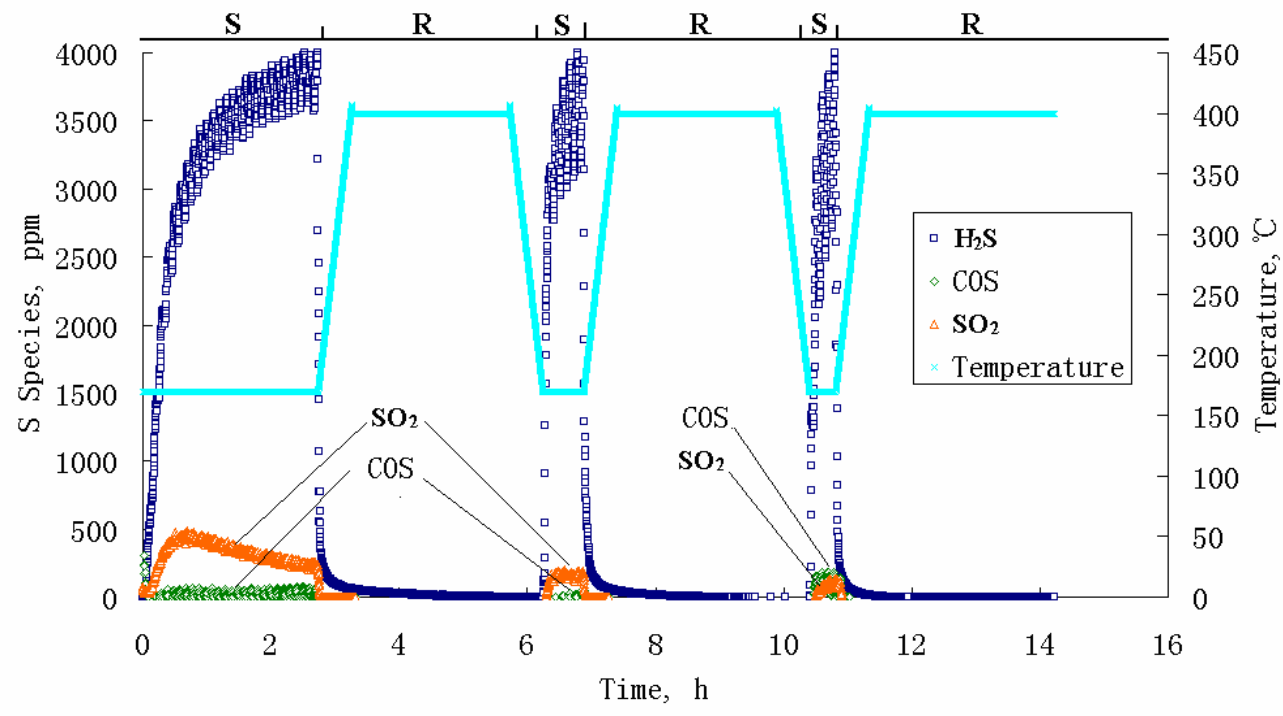

Figure 26. Sulfurization (S) and regeneration (R) of ACF- $LaCl_3$-NaOH under wet condition**.** Sulfurization with 4000 ppm H_2S at 170 ºC, when effluent H_2S concentration

reached 4000 ppm, simulated syngas was switched to N_2, and temperature was increased to 400 ºC for regeneration of sorbent. Then temperature was decreased to 170 ºC and another sulfurization and regeneration cycle began. By-produce including COS and SO_2 were also investigated.

The performance of ACF- $LaCl_3$-NaOH sorbent for three cycles is shown in Figure 26. The capacity of H_2S uptake in the 1st cycle was 14 mg H_2S/g Sorbent or 3.6 mg H_2S/cm^3-Sorbent, which was 63% higher than that of original ACF only volume basis since the density of additive was higher than that of ACF but the total volume of modified sorbent was not different from the original volume of ACF only. Although the surface area of the sorbent was much smaller after modification, the even better H_2S-uptake capacity was related to the presence of $La(OH)_3$. Possible reaction mechanisms are shown below [60]:

$$3\ H_2S + La(OH)_3 \rightarrow La(HS)_3 + 3\ H_2O$$

$$3\ H_2S + 2\ La(OH)_3 \rightarrow La_2S_3 + 6\ H_2O$$

The appearance of black metal-brightness substance retained on the wall of the reactor supports the hypothesis postulating the formation of metal sulfide. Surface oxidation reactions that result in formation of elemental sulfur or sulfur dioxide, and further oxidation to H_2SO_4 are shown as below:

$$2\ H_2S + O_2 \rightarrow 2\ S + 2\ H_2O$$

$$2\ H_2S + 3\ O_2 \rightarrow 2\ SO_2 + 2\ H_2O \quad \text{or} \quad S + O_2 \rightarrow SO_2$$

$$2\ SO_2 + 2\ H_2O + O_2 \rightarrow 2\ H_2SO_4$$

4.5.4 Sulfur Byproducts

During the sulfurization of all materials evaluated in this study, COS and SO_2 were monitored as possible byproducts and the corresponding example results are shown in the Figure 23 through Figure 26. It was observed in all cases that COS shows up early and increases to the maximum value during half an hour after the sulfurization began in the 1st cycle. The formation of COS is attributed to the reaction of H_2S and CO [63], which may happen inside the inlet tubing [3] before the gas mixture is introduced to the reactor. In the 2nd and 3rd cycles of Figure 24 and Figure 25, the COS peak shows up immediately after the gas mixture switched from N_2 to simulated syngas. Because when syngas was switched to N_2 by turning a 3-way valve, the previous residual syngas in the tubing was not vented and COS was likely formed. This explains the appearance of COS in the early period during the process and it was not reliably preventable. Another way to form COS is that CO reacts with elemental sulfur. When elemental sulfur is formed on the surface of sorbents through H_2S oxidation, it is possible that sulfur reacts with CO in the syngas or with other carbon-oxygen complexes to form COS [3]. As elemental sulfur is further oxidized to SO_2 or SO_4^{2-}, the formation of COS decreases with the decrease of elemental sulfur. In Figure 25 and Figure 26, COS remains a constant at a low level during the process possibly because hydroxide could counteract the formation of COS, as shown below [64,65].

$$COS + 4\ OH^- \rightarrow CO_3^{2-} + S^{2-} + 2\ H_2O$$

The emissions of SO_2 during the sulfurization of ACF and ACF-$LaCl_3$ were lower (< 100 ppm), compared to that with ACF-La_2O_3-NaOH.and ACF- $LaCl_3$-NaOH sorbents (< 500 ppm). ACF has much higher surface area and pore volume compared to other sorbents so that water film could be easily formed and SO_2 is more likely to be further oxidized to sulfate. In the

same way, abundant water film which promotes capture of SO_2 is formed on the surface of the ACF-$LaCl_3$ due to strong water adsorption by $LaCl_3$, as summarized below:

$$SO_2 + H_2O \rightarrow H_2SO_3$$

$$SO_2 + O_2 + H_2O \rightarrow SO_4^{2-} + 2\ H^+$$

ACF-La_2O_3-NaOH and ACF-$LaCl_3$-NaOH were supposed to have better capability to adsorb SO_2 due to hydroxide presence. However, more SO_2 was released from these sorbent which may be attributed to: 1) most of the pores were occupied by additive compounds so that water could not be captured on the surface; 2) competition from the other two sulfur species (H_2S and COS).

5.0 SUMMARY AND CONCLUSIONS

Carbon black and graphite have small surface area (1 – 225 m^2/g) and higher quantity of acidic functional groups (32 – 77%) so in order to be effective in removal of H_2S they might need heat pretreatment or basicity modification. Activated carbon fibers exhibited very good performance for H_2S removal (as high as 32 mg H_2S/g Sorbent) and deserve more attention in the research and application of H_2S removal.

The conclusion that higher quantity and/or ratio of basic functionalities leads to higher capacity of H_2S uptake is still tenable in terms of different kinds of carbonaceous materials. Possible reactions between basic functional groups and H_2S are proposed.

Sulfurization of carbon materials at the temperature ranging from 110 to 170 °C under humid condition was found to lead to higher capacity for H_2S uptake possibly because it offer optional conditions for physical adsorption and chemisorption and better water film distribution on the sorbent surface. Measured activation energy of desorption of sulfur species on sulfurized carbon materials demonstrates that chemisorption plays the main role in desulfurization at higher temperature while physical adsorption is the dominant process at lower temperature.

The combinations of high-adsorption-efficiency activated carbon fibers with regenerative rare earth metal compounds to remove H_2S from simulated syngas were determined. Compared to original ACFs, higher H_2S-uptake capacity was obtained with lanthanum-modified ACF sorbents during the initial cycle, showing promising potential to remove H_2S.

Lower H_2S uptake capacities in the 2nd and 3rd cycles were due to the fact that N_2 was the only gas for regeneration of sorbent. If O_2 were used instead, the metal sulfide could be oxidized in the regeneration cycle. In this set of experiments, it was observed that N_2 only flushed out physically adsorbed H_2S and volatile elemental sulfur gas but it cannot remove chemically adsorbed sulfur.

To improve sulfur removal efficiency and decrease the formation of undesired by-products, it is better to shorten the mixing time of H_2S and CO because they could form COS when giving enough time under a certain temperature.

6.0 FUTURE WORK

To investigate and isolate the exact reactions on the surface of sorbent, diffuse reflectance infrared Fourier transform spectroscopy (DRIFTS) could be used to investigate the compounds that are formed on the surface of carbonaceous material. Scanning Electron Microscope and Energy Dispersive Analysis X-ray (SEM-EDAX) could also be used to identify products retained, which would help to explain reaction mechanisms and dynamics.

In terms of regeneration of carbonaceous sorbents, gas mixtures containing CO, CO_2, H_2O, H_2 and N_2 without O_2 (carbon is oxidized or combusts in the presence of O_2 at high temperature) could be used to perform regeneration experiments because metal sulfide formed could be oxidized back to metal oxide. The gas mixture may remove chemically adsorbed H_2S without eliminating carbon sorbent.

Increasing H_2S removal efficiency and reducing undesired by-products also should be paid attention to. Most researchers only focused on H_2S and avoided to talk about or did not investigate by-product (COS and SO_2) in the tail gas after desulfurization at the same time whereas SO_2 is also a kind of corrosive gas and COS is a threat due to its toxicity.

APPENDIX

FIGURES AND TABLE RELATED TO SULFURIZATION AND TGA EXPERIMENT

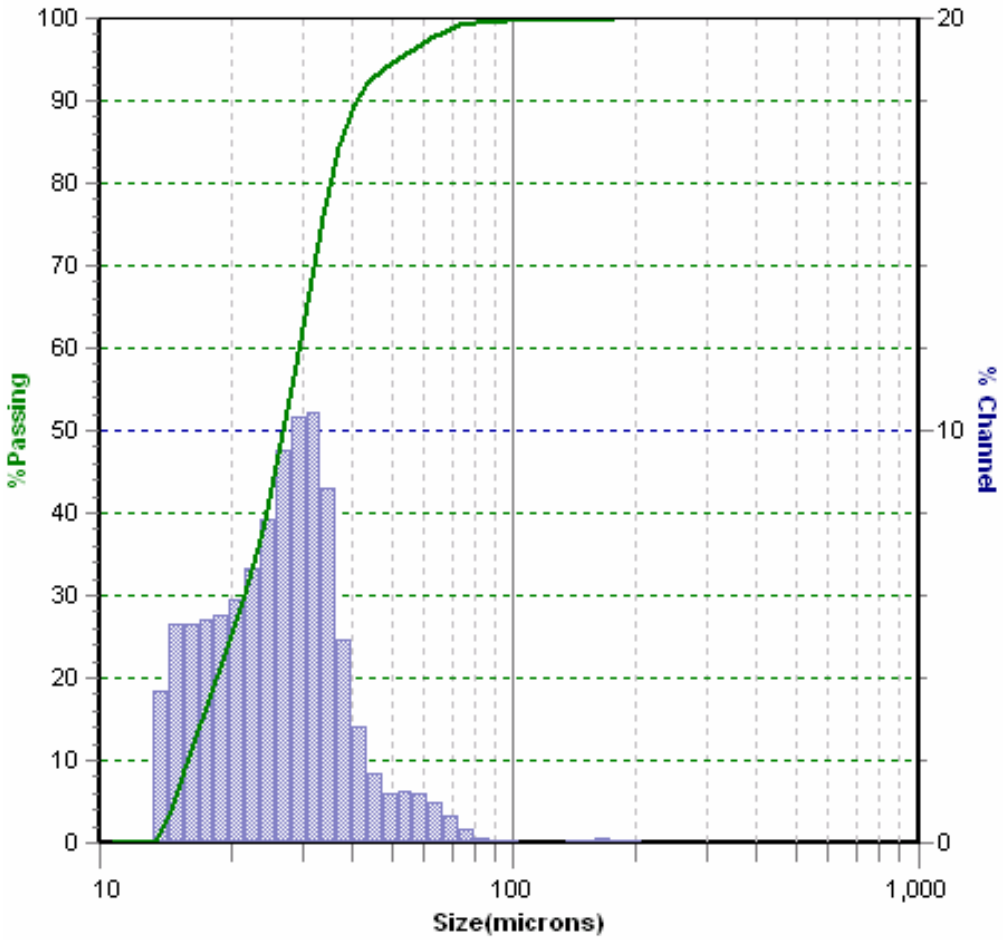

Figure 27. Particle size and distribution of ACF10 (0.75 – 228 μm) with an average particle diameter 27 μm.

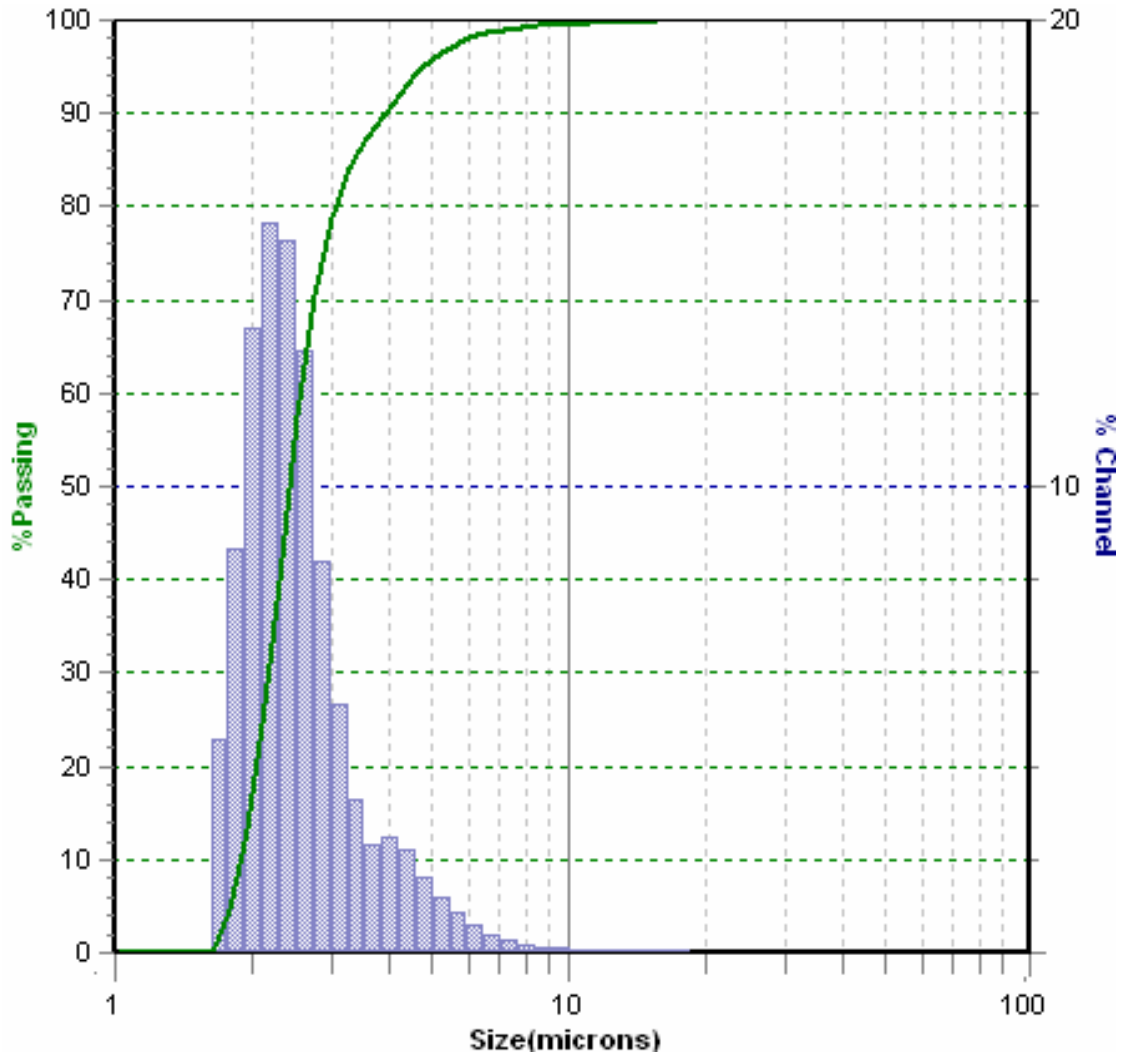

Figure 28. Particle size and distribution of CeO_2 (1.8 – 23 μm) with an average particle diameter 2.4 μm.

Table 10. Functionalities on the surface of carbon blacks and graphite. Acidic functional groups were specified by Boehm titration.

Sample	Total Acidity, m mol/g	Carboxylic m mol/g	Lactone m mol/g	Phenolic m mol/g	Carbonyl m mol/g	Basicity m mol/g
BP460	0.58	0.167	0.0558	0.0213	0.336	0.186
BP800	0.57	0.148	0.025	0.0104	0.387	0.136
Graphite	0.195	0.0557	0.104	0.0285	0.00636	0.124

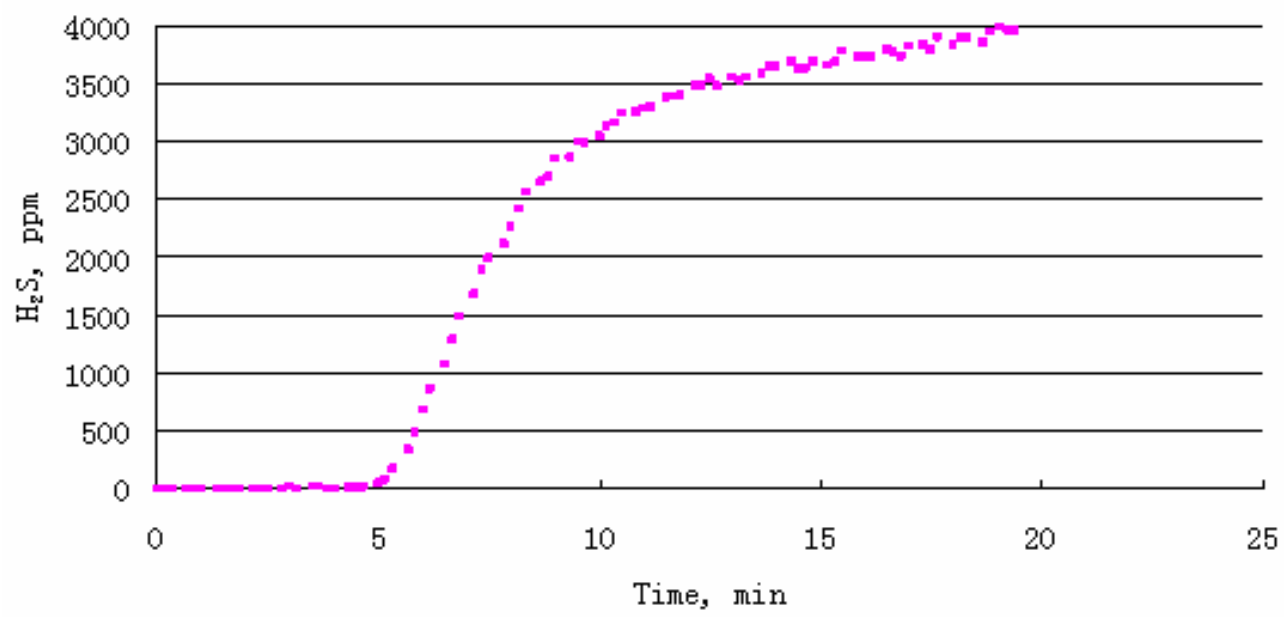

Figure 29. Sulfurization of ACF 10 with simulated syngas whose ratio of H_2S and O_2 is 1 : 2 at room temperature with 4000 ppm H_2S under dry condition.

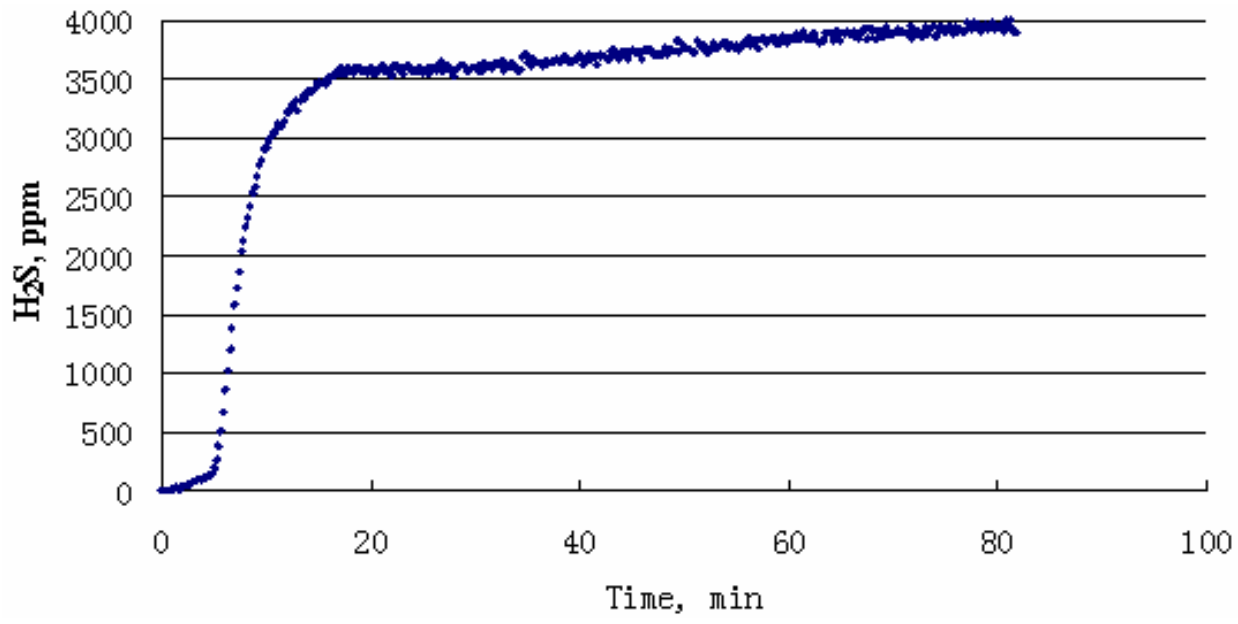

Figure 30. Sulfurization of dry mixed sorbents of ACF and CeO_2 at room temperature with 4000 ppm H_2S under dry condition, with capacity of 8.06 mg H_2S/g Sorbent

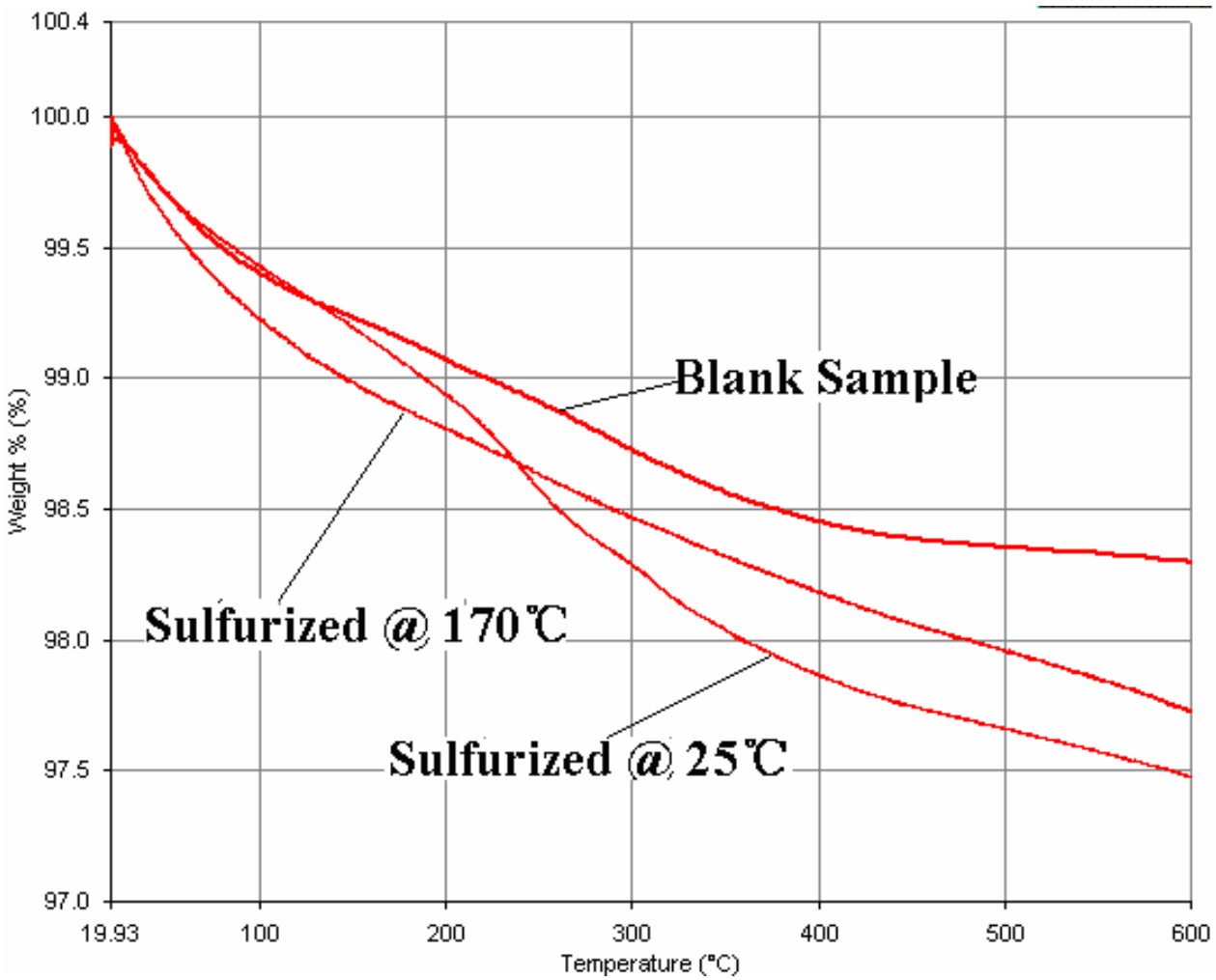

Figure 31. TGA runs of fresh ACF10 without sulfurization and ACF10 after sulfurization. Sulfide samples had more weight loss due to sulfur species retained after sulfurization.

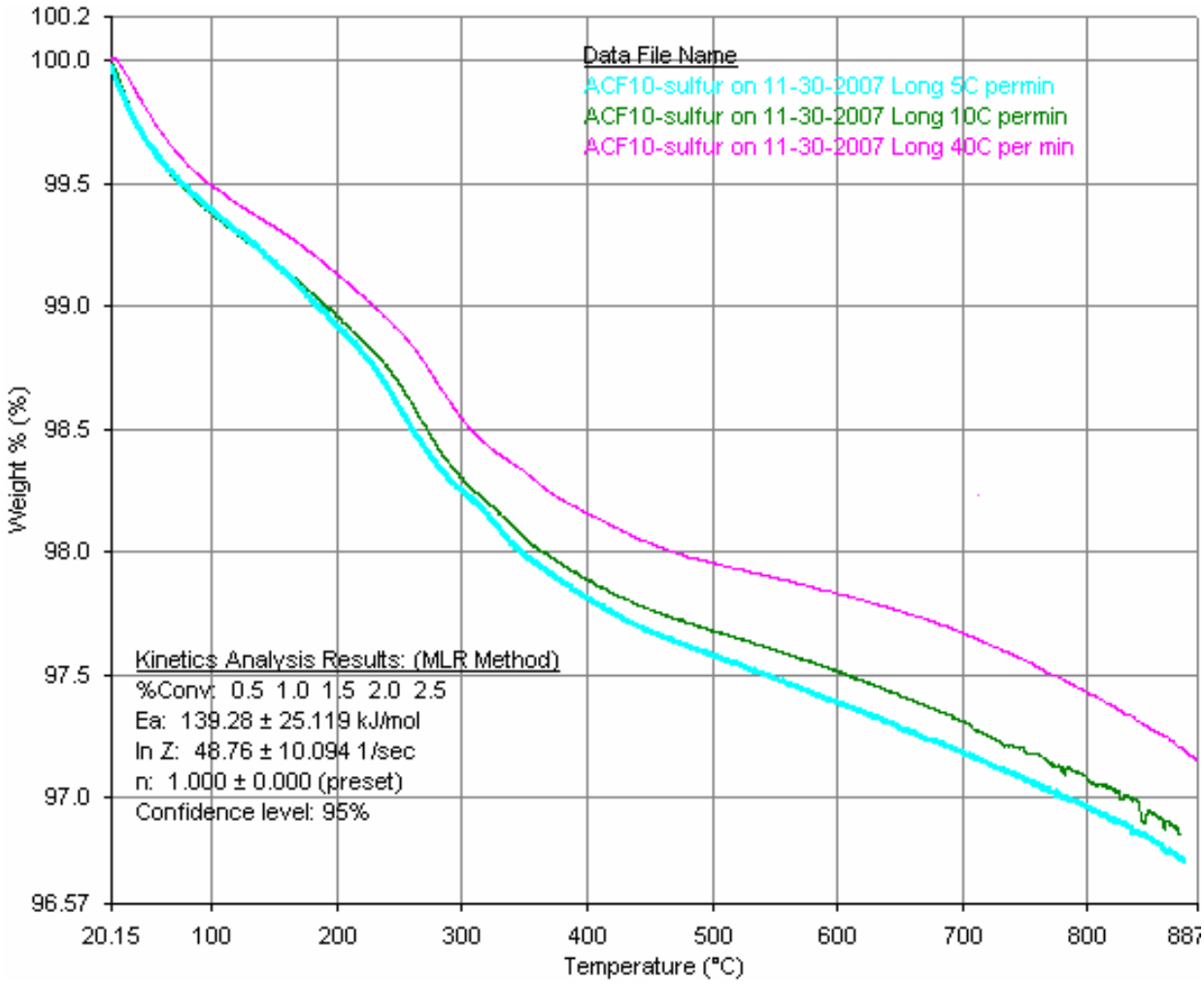

Figure 32. TGA kinetic analysis of ACF10 sulfurized at 25 ºC. The weight loss curve shifted at different scan rate to determine the activation energy of sulfur species (result is shown in Page 64).

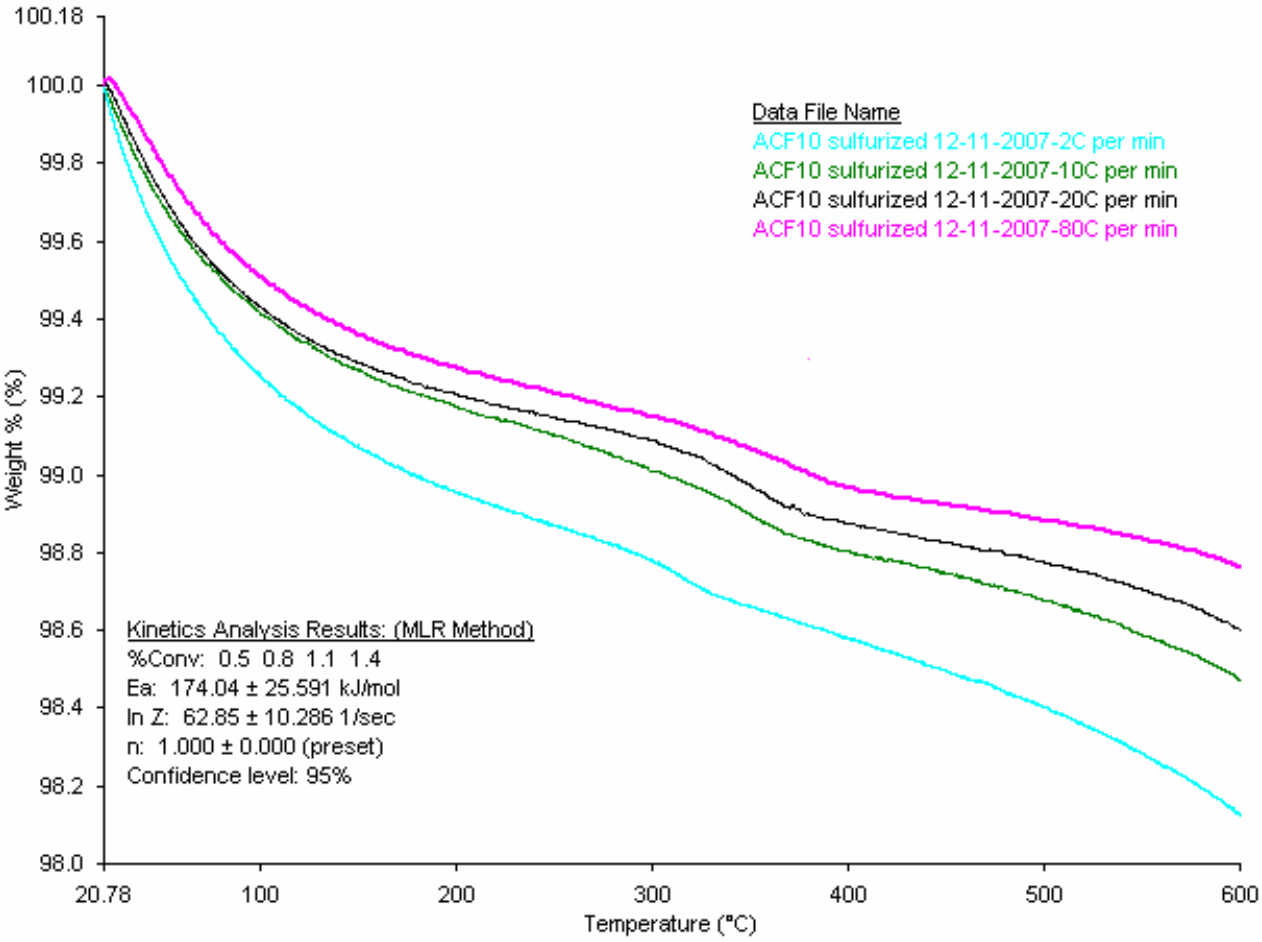

Figure 33. TGA kinetic analysis of ACF10 sulfurized at 110 ºC. The weight loss curve shifted at different scan rate to determine the activation energy of sulfur species (result is shown in Page 64).

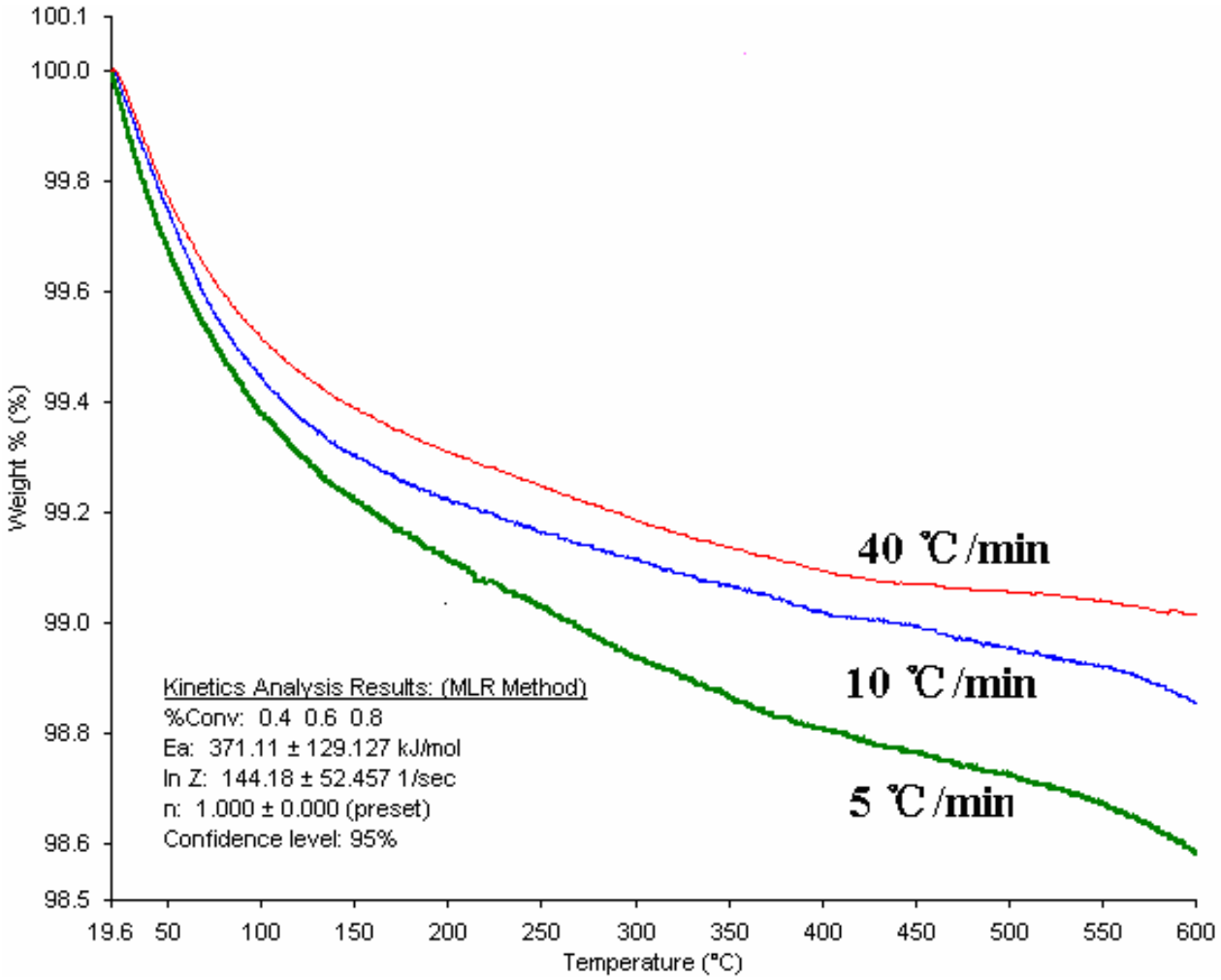

Figure 34. TGA kinetic analysis of ACF10 sulfurized at 210 ºC. The weight loss curve shifted at different scan rate to determine the activation energy of sulfur species (result is shown in Page 64).

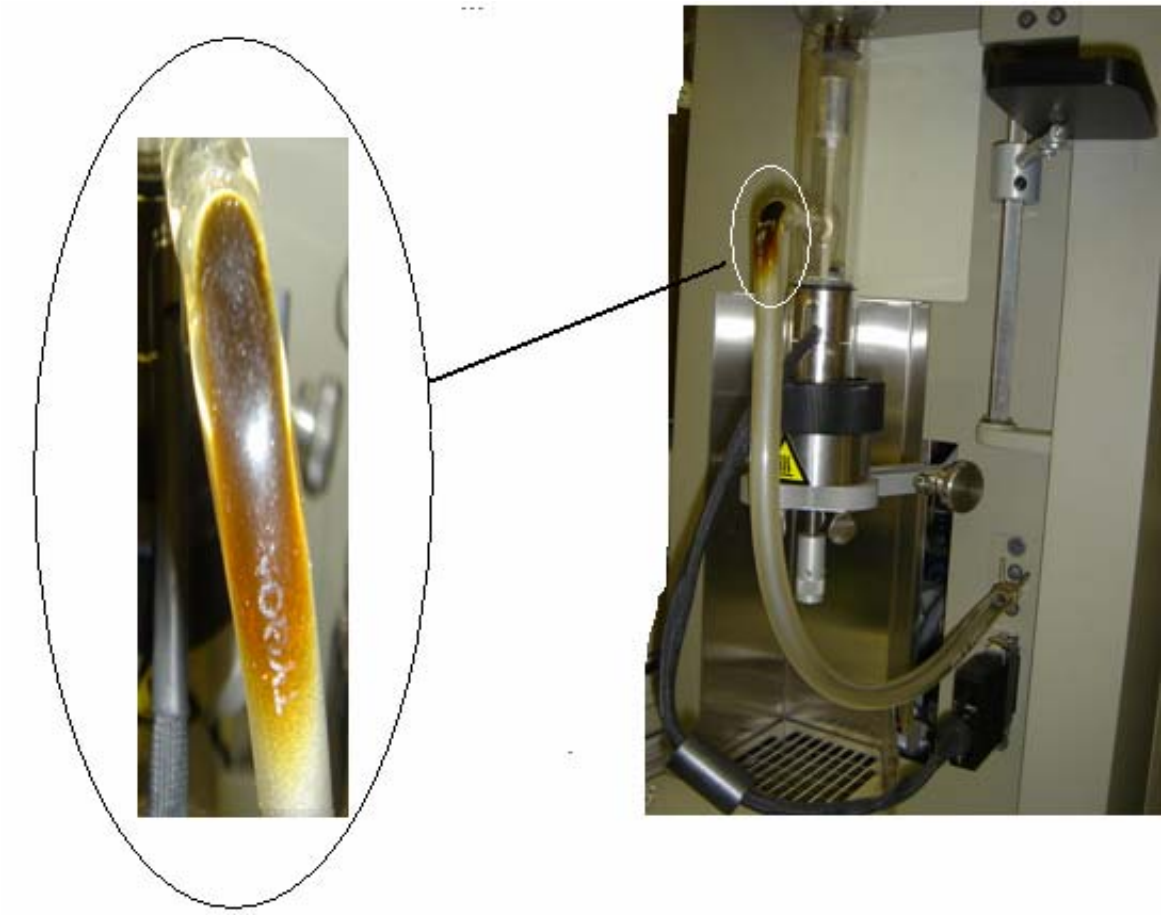

Figure 35. Yellow elemental sulfur desorbed from sulfurized ACF10 samples accumulated at the outlet of the tube of TGA

BIBLIOGRAPHY

1. Chauk SS, Agnihotri R, Jadhav RA, Misro SK, Fan L-S: Kinetics of high-pressure removal of hydrogen sulfide using calcium oxide powder. AIChE Journal 2000;46:1157.

2. Eow JS: Recovery of sulfur from sour acid gas: A review of the technology. Environmental Progress 2002;21:143.

3. Wu X, Schwartz V, Overbury SH, Armstrong TR: Desulfurization of gaseous fuels using activated carbons as catalysts for the selective oxidation of hydrogen sulfide. Energy and Fuels 2005;19:1774.

4. Wikipedia: Integrated Gasification Combined Cycle. http://en.wikipedia.org/wiki/Igcc Date accessed: April 4, 2008

5. Hee Kwon J, Tae Jin L, Si Ok R, Jae Chang K: A study of Zn - Ti-based H_2S removal sorbents promoted with cobalt oxides. Industrial and Engineering Chemistry Research 2001;40:3547.

6. Ko T-H, Chu H, Chaung L-K: The sorption of hydrogen sulfide from hot syngas by metal oxides over supports. Chemosphere 2005;58:467.

7. Tsai J-H, Jeng F-T, Chiang H-L: Removal of H2S from exhaust gas by use of alkaline activated carbon. Adsorption 2001;7:357.

8. Davini P: Flue gas desulphurization by activated carbon fibers obtained from polyacrylonitrile by-product. Carbon 2003;41:277.

9. Huang C-C, Chen C-H, Chu S-M: Effect of moisture on H_2S adsorption by copper impregnated activated carbon. Journal of Hazardous Materials 2006;136:866.

10. Lawrence NS, Deo RP, Wang J: Electrochemical determination of hydrogen sulfide at carbon nanotube modified electrodes. Analytica Chimica Acta 2004;517:131.

11. Wikipedia: http://en.wikipedia.org/wiki/Hydrogen_sulfide. Date accessed: April 4, 2008

12. Shooter D: Sources and sinks of oceanic hydrogen sulfide - an overview. Atmospheric Environment 1999;33:3467.

13. Burstyn I, Senthilselvan A, Kim H-M, Cherry NM, Pietroniro E, Waldner C: Industrial sources influence air concentrations of hydrogen sulfide and sulfur dioxide in rural areas of Western Canada. Journal of the Air and Waste Management Association 2007;57:1241.

14. Cal MP, Strickler BW, Lizzio AA: High temperature hydrogen sulfide adsorption on activated carbon - I. Effects of gas composition and metal addition. Carbon 2000;38:1757.

15. Iyoha O, Enick R, Killmeyer R, Howard B, Ciocco M, Morreale B: H_2S production from simulated coal syngas containing H_2S in multi-tubular Pd and 80 wt% Pd-20 wt% Cu membrane reactors at 1173 K. Journal of Membrane Science 2007;306:103.

16. Mary Anne Alvin RS, Richard A. Newby, Dale L. Keairns: Selective Catalytic Oxidation of Hydrogen Sulfide — IGCC Applications. 23rd International Pittsburgh Coal Conference, Pittsburgh, PA September 2006.

17. Wikipedia: Claus process. http://en.wikipedia.org/wiki/Claus_process. Date accessed: April 4, 2008

18. Li K-T, Chi Z-H: Effect of antimony oxide on magnesium vanadates for the selective oxidation of hydrogen sulfide to sulfur. Applied Catalysis B: Environmental 2001;31:173.

19. Pena JM, Allen NS, Edge M, Liauw CM, Hoon SR, Valange B, Cherry RI: Analysis of radical content on carbon black pigments by electron spin resonance: Influence of functionality, thermal treatment and adsorption of acidic and basic probes. Polymer Degradation and Stability 2000;71:153.

20. Wikipedia: http://en.wikipedia.org/wiki/Graphite. Date accessed: April 4, 2008

21. Kwon S, Vidic R, Borguet E: Enhancement of adsorption on graphite (HOPG) by modification of surface chemical functionality and morphology. Carbon 2002;40:2351.

22. Adib F, Bagreev A, Bandosz TJ: Adsorption/oxidation of hydrogen sulfide on nitrogen-containing activated carbons. Langmuir 2000;16:1980.

23. Bagreev A, Adib F, Bandosz TJ: pH of activated carbon surface as an indication of its suitability for H2S removal from moist air streams. Carbon 2001;39:1897.

24. Bandosz TJ: Effect of pore structure and surface chemistry of virgin activated carbons on removal of hydrogen sulfide. Carbon 1999;37:483.

25. Shin C, Kim K, Choi B: Deodorization technology at industrial facilities using impregnated activated carbon fiber. Journal of Chemical Engineering of Japan 2001;34:401.

26. Bagreev A, Bandosz TJ: A role of sodium hydroxide in the process of hydrogen sulfide adsorption/oxidation on caustic-impregnated activated carbons. Industrial and Engineering Chemistry Research 2002;41:672.

27. Li Z, Flytzani-Stephanopoulos M: Cu-Cr-O and Cu-Ce-O Regenerable Oxide Sorbents for Hot Gas Desulfurization. Industrial & Engineering Chemistry Research 1997;36:187-196.

28. Bukhtiyarova GA, Delii IV, Sakaeva NS, Kaichev VV, Plyasova LM, Bukhtiyarov VI: Effect of the calcination temperature on the properties of Fe_2O_3/SiO_2 catalysts for oxidation of hydrogen sulfide. Reaction Kinetics and Catalysis Letters 2007;92:89.

29. Li K-T, Chi Z-H: Selective oxidation of hydrogen sulfide on rare earth orthovanadates and magnesium vanadates. Applied Catalysis A: General 2001;206:197.

30. Flytzani-Stephanopoulos M, Sakbodin M, Wang Z: Regenerative adsorption and removal of H_2S from hot fuel gas streams by rare earth oxides. Science 2006;312:1508.

31. Nguyen-Thanh D, Bandosz TJ: Activated carbons with metal containing bentonite binders as adsorbents of hydrogen sulfide. Carbon 2005;43:359.

32. Rosso I, Galletti C, Bizzi M, Saracco G, Specchia V: Zinc oxide sorbents for the removal of hydrogen sulfide from syngas. Industrial and Engineering Chemistry Research 2003;42:1688.

33. Nakamura T, Kawasaki N, Hirata M, Oida Y, Tanada S: Adsorption of hydrogen sulfide by zinc-containing activated carbon. Toxicological and Environmental Chemistry 2001;82:93.

34. Bouzaza A, Laplanche A, Marsteau S: Adsorption-oxidation of hydrogen sulfide on activated carbon fibers: Effect of the composition and the relative humidity of the gas phase. Chemosphere 2004;54:481.

35. Cal MP, Strickler BW, Lizzio AA, Gangwal SK: High temperature hydrogen sulfide adsorption on activated carbon - II. Effects of gas temperature, gas pressure and sorbent regeneration. Carbon 2000;38:1767.

36. Jensen AB, Webb C: Treatment of H_2S-containing gases: a review of microbiological alternatives. Enzyme and Microbial Technology 1995;17:2.

37. Melo DMA, De Souza JR, Melo MAF, Martinelli AE, Cachima GHB, Cunha JD: Evaluation of the zinox and zeolite materials as adsorbents to remove H_2S from natural gas. Colloids and Surfaces A: Physicochemical and Engineering Aspects 2006;272:32.

38. Demmink JF, Beenackers AACM: Gas desulfurization with ferric chelates of EDTA and HEDTA: New model for the oxidative absorption of hydrogen sulfide. Industrial & Engineering Chemistry Research 1998;37:1444.

39. Limtrakul S, Rojanamatin S, Vatanatham T, Ramachandran PA: Gas-lift reactor for hydrogen sulfide removal. Industrial and Engineering Chemistry Research 2005;44:6115.

40. Bashkova S, Baker FS, Wu X, Armstrong TR, Schwartz V: Activated carbon catalyst for selective oxidation of hydrogen sulphide: On the influence of pore structure, surface characteristics, and catalytically-active nitrogen. Carbon 2007;45:1354.

41. Le Leuch LM, Subrenat A, Le Cloirec P: Hydrogen sulfide adsorption and oxidation onto activated carbon cloths: Applications to odorous gaseous emission treatments. Langmuir 2003;19:10869.

42. Ishii C, Suzuki T, Shindo N, Kaneko K: Structural characterization of heat-treated activated carbon fibers. Journal of Porous Materials 1997;4:181.

43. Feng W: Hydrogen Sulfide Adsorption/Oxidation on Carbonaceous Surfaces and Its Application in Vapor Phase Mercury Control. Dissertation, University of Pitssburgh 2005.

44. Kastner JR, Buquoi Q, Melear ND, Das KC: Low temperature catalytic oxidation of hydrogen sulfide and methanethiol using wood and coal fly ash. Environmental Science and Technology 2003;37:2568.

45. Feng X, Dementev N, Feng W, Vidic R, Borguet E: Detection of low concentration oxygen containing functional groups on activated carbon fiber surfaces through fluorescent labeling. Carbon 2006;44:1203.

46. Beck NV, Meech SE, Norman PR, Pears LA: Characterisation of surface oxides on carbon and their influence on dynamic adsorption. Carbon 2002;40:531.

47. Mohtadi R, Lee WK, Van Zee JW: The effect of temperature on the adsorption rate of hydrogen sulfide on Pt anodes in a PEMFC. Applied Catalysis B: Environmental 2005;56:37.

48. Sun J, Modi S, Liu K, Lesieur R, Buglass J: Kinetics of zinc oxide sulfidation for packed-bed desulfurizer modeling. Energy and Fuels 2007;21:1863.

49. Boehm HP: Surface Oxides of Carbon. Angewandte Chemie International Edition 1964;3:669.

50. Boehm HP: Functional Groups on the Surface of Solids. Angewandte Chemie International Edition 1966;5:533-622.

51. Boehm HP: Some aspects of the surface chemistry of carbon blacks and other carbons. Carbon 1994;32:759.

52. PerkinElmer: Pyris Kinetics Software Guide. TGA 7 Manuals;Pyris™ Software Release Notes for Version 7.0.

53. Gurrath M, Kuretzky T, Boehm HP, Okhlopkova LB, Lisitsyn AS, Likholobov VA: Palladium catalysts on activated carbon supports. Influence of reduction temperature, origin of the support and pretreatments of the carbon surface. Carbon 2000;38:1241.

54. Adib F, Bagreev A, Bandosz TJ: Analysis of the relationship between H₂S removal capacity and surface properties of unimpregnated activated carbons. Environmental Science and Technology 2000;34:686.

55. Feng W, Kwon S, Borguet E, Vidic R: Adsorption of hydrogen sulfide onto activated carbon fibers: Effect of pore structure and surface chemistry. Environmental Science and Technology 2005;39:9744.

56. Choi JJ, Hirai M, Shoda M: Catalytic oxidation of hydrogen sulphide by air over an activated carbon fibre. Applied Catalysis 1991;79:241.

57. Flytzani-Stephanopoulos M, Sakbodin M, Wang Z: Regenerative Adsorption and Removal of H_2S from Hot Fuel Gas Streams by Rare Earth Oxides. Science (Washington, DC, United States) 2006;312:1508-1510.

58. Dean JA: Lange's Chemistry Handbook Version 15th. 1998.

59. Moshfegh AZ, Zakeri KH: The kinetic study of H_2S formation and desorption on the S/Pt(111) surface by computer simulation. Surface Review and Letters 2003;10:745.

60. Yan R, Liang DT, Tsen L, Tay JH: Kinetics and mechanisms of H_2S adsorption by alkaline activated carbon. Environmental Science and Technology 2002;36:4460.

61. Qiao Z-J, Li J-J, Zhao N-Q, Wei N: Pore size and surface properties of activated carbon fibres modified by high temperature treatment. Xinxing Tan Cailiao/New Carbon Materials 2004;19:53.

62. Dugulan AI, Hensen EJM, van Veen JAR: High-pressure sulfidation of a calcined $CoMo/Al_2O_3$ hydrodesulfurization catalyst. Catalysis Today 2008;130:126.

63. Ko T-H, Chu H, Lin H-P, Peng C-Y: Red soil as a regenerable sorbent for high temperature removal of hydrogen sulfide from coal gas. Journal of Hazardous Materials 2006;136:776.

64. Bhave RR, Sharma MM: Extraction of COS dissolved in n-Heptane into aqueous sodium hydroxide: phase transfer catalysis. Chemical Engineering Science 1983;38:141.

65. Chaudhuri SK, Sharma MM: Absorption of carbonyl sulfide in aqueous alkaline solutions: New strategies. Industrial & Engineering Chemistry Research 1989;28:870.